2015

Characterizing the nuclear import and functions of cystin, the ciliary protein disrupted in the cpk mouse model of recessive polycystic kidney disease

Jacob Asher Watts
University of Alabama at Birmingham

CHARACTERIZING THE NUCLEAR IMPORT AND FUNCTIONS OF CYSTIN, THE CILIARY PROTEIN DISRUPTED IN THE *CPK* MOUSE MODEL OF RECESSIVE POLYCYSTIC KIDNEY DISEASE

by

JACOB ASHER WATTS

LISA GUAY-WOODFORD, COMMITTEE CHAIR
KAI JIAO
PAUL SANDERS
DAVID SCHNEIDER
BRADLEY YODER

A DISSERTATION

Submitted to the graduate faculty of The University of Alabama at Birmingham
in partial fulfillment of the requirements for the degree of
Doctor of Philosophy

BIRMINGHAM, ALABAMA

2015

CHARACTERIZING THE PATHWAYS FOR INTERACELLUAR TRAFFICKING AND NUCLEAR FUNCTION OF CYSTIN USING TANDEM AFFINITY PURIFICATION

JACOB ASHER WATTS

GENETICS, GENOMICS, AND BIOINFORMATICS

ABSTRACT

Autosomal recessive polycystic kidney disease (ARPKD; MIM 263200) is a major cause of pediatric morbidity and mortality. Typically, orthologous animal models are the mainstay for pathogenic studies of human diseases. However, gene-targeting of *Pkhd1*, the mouse ortholog of the ARPKD gene, results in mutants with little or no kidney disease. In contrast, disruption of the non-orthologous gene, *Cys1*, in the *cpk* mouse model closely phenocopies human ARPKD. We speculate that this phenotypic similarity suggests that the *Pkhd1* and *Cys1* genes encode proteins (FPC and cystin, respectively) that share, at least in part, common molecular pathways. Our laboratory, as well as others, has shown that both proteins are cilia-associated and involved in regulated trafficking from the cilia to the nucleus, where they modulate specific gene transcription.

The current study was designed to identify cystin-binding partners and characterizing the pathways for cystin intracellular trafficking and nuclear function. To identify interacting partners, we undertook an agnostic approach using tandem affinity purification (TAP). A stable mIMCD-3 cell line was generated expressing a cystin TAP construct. TAP was performed (n=4) on cell lysate from cells grown to optimize cilia expression. A combination of SDS-PAGE, Spyro Ruby staining, western blotting, and mass spectrometry was used to identify putative interacting partners. GST-pulldown experiments have confirmed a direct interaction between cystin and Importin α1, Importin α2,

and Importin β2. We also present data that implicates cystin in the regulation of *Pkhd1* splicing. Finally, we were able to identify and characterize a novel functional interaction between cystin and the ciliary GTPase, Arl3.

Together, these data extend our initial observations regarding cystin interactions and implicate its function in cilia-associated and nuclear transport-related protein complexes. Taken together, these data suggest that cystin and its putative interacting partners e.g., Arl3, define one or more protein complexes and/or pathways that are critical for renal tubular homeostasis and are involved in recessive PKD pathogenesis.

Keywords: cystoproteins, cystin, tandem affinity purification (TAP), trafficking, polycystic kidney disease, cilia

ACKNOWLEDGMENTS

Firstly, I must express my sincerest appreciation and gratitude for my mentor, teacher, and friend, Lisa Guay-Woodford. I consider myself very fortunate to have been a part of her laboratory throughout my time in graduate school. She leads her team with loyalty, dedication, humor, integrity, and warmth that make you feel you are part of something truly special. Her support, passion, determination, and willingness to help others have been an inspiration. She has left an indelible mark on both my personal and professional lives for which I am truly thankful.

Next I would like to thank the members of my committee: Drs. Brad Yoder, Kai Jiao, Paul Sanders, and David Schneider. Their guidance and suggestions have helped me to navigate a challenging project and gave me the confidence and motivation I needed to achieve my goals.

I am enormously thankfully for the members of the Guay-Woodford laboratory group, both past and present. Working with such wonderfully talented people has been a gift. The collaborative nature of our lab has allowed me not only to learn, but also to thrive and has helped shape me into the scientist that I am today. I also want to thank all of the important people who work tirelessly behind the scenes to keep everything running smoothing including Drs. Bullard, Jiao, Elgavish, Nan Travis, and Scott Austin for all of their hard work and support. I would also like to thank Mozella Kerley, who is always there to greet you with a warm smile and an encouraging word. She is indeed a bright light to all who know her.

I have to thank all of my friends who have supported me through this experience. Firstly, thanks to Erica Hernandez, for being the best of friends, a confidant, therapist, HLP, and everything in between. I would be lost without our friendship and I'm so thankful that you are still here after all of these years. To Jayne Ellis, for encouraging me to pursue a graduate education. To Monica Nguyen, Caitlin Traylor, Kevin & Whittany Starns, Scott Padgett, and Noushin & Titus Cline, thank you for welcoming me home with smiling faces and open arms at every visit. You are all the best friends I could ask for, even if you make fun of how long I've been in school. I am also extremely grateful to my fellow students at UAB, particularly Michelle McClure, Paige DeBenedittis, Cris Harmelink, Emily Spencer, Brandon Shaw, Arindam Ghosh, and Louisa Pyle who have been such wonderful friends and an invaluable support system, both personally and professionally. They made Birmingham feel more like home.

Most importantly I must thank my family, especially my parents, Billy and Sheila Watts, who have always supported me and stood behind me. Your support, love, and encouragement have always meant the world to me. Knowing that I always have a safe place to land has allowed me to achieve things I never dreamed were possible. From a small town in Louisiana to earning my Ph.D. in Washington, DC - a journey that would not have been possible without you all. I love you more than I can ever say. Finally, even though they are no longer with us, I must thank my grandparents, Joe & Maxine Pine. You are gone from us, but your presence and love, which helped to shape our family, are still felt every day. I miss you, Mena and Grandad.

"When someone is in your heart, they're never truly gone; they can come back to you, even at unlikely times." – Mitch Album, *For One More Day*

TABLE OF CONTENTS

Page

LIST OF TABLES

Table *Page*

INTRODUCTION

TANDEM AFFINITY PURIFICATION OF CYSTIN, THE CILIARY PROTEIN DISRUPTED IN THE *CPK* MODEL OF POLYCYSTIC KIDNEY DISEASE, SUGGESTS ITS ROLE IN SPLICING REGULATION OF *PKHD1*

LIST OF FIGURES

Figure *Page*

INTRODUCTION

TANDEM AFFINITY PURIFICATION OF CYSTIN, THE CILIARY PROTEIN DISRUPTED IN THE *CPK* MODEL OF POLYCYSTIC KIDNEY DISEASE, SUGGESTS ITS ROLE IN SPLICING REGULATION OF *PKHD1*

CRISPR-MEDIATED KNOCKDOWN OF ARL3 REVEALS A FUNCTIONAL INTERACTION WITH CYSTIN, THE CILIARY PROTEIN DISRUPTED IN THE *CPK* MOUSE MODEL OF RECESSIVE POLYCYSTIC KIDNEY DISEASE

CHAPTER 1

INTRODUCTION

Primary Cilia and the Ciliopathies

Primary cilia are small, evolutionarily conserved, membrane-bound organelles projecting from most eukaryotic cell types. The cilium is structurally subdivided into different compartments: the basal body, the transition zone, axoneme, as well as the ciliary membrane, and the tip (Figure 1.1)[1]. The cilium emanates from the basal body, a modified centriole anchored to the apical plasma membrane and protrudes from the surface of the cell contiguous with the plasma membrane. Although the ciliary membrane is continuous with the cellular plasma membrane, it contains its own coterie of proteins and a unique lipid composition[2, 3]. The core of the cilium consists of a highly organized axoneme made up of microtubule doublets that extend from the basal body, which served as a ballast, securing the axoneme to the cell[4, 5].

Multiple studies have demonstrated that the cilium is a hub of signaling activity, playing a role in several pathways including hedgehog, mammalian target of rapamycin (mTOR), and possibly canonical and noncanonical Wnt signaling[6]. Primary cilia have many different important functions, including left-right developmental patterning, as well as serving as mechanosensors, photosensors, and chemosensors, responding to various stimuli, such as luminal flow in the adult kidney, and eliciting a response within the cell[7-13]. A number of proteins associated with renal cystic disease, such as polycystin-1, polycystin-2, fibrocystin/polyductin complex (FPC), Ift88 and cystin have been

demonstrated to localize to the primary cilium in renal epithelial cells (Figure 1.2)[14, 15]. Structural or functional disruptions in the cilium result in a group of disorders referred to as the ciliopathies[16-18]. The term ciliopathies is a broad classification, encompassing a diverse group of disorders with a wide array of phenotypic presentations. However, a subset of the ciliopathies present with renal cystic disease as well as portobiliary tract dysgenesis. These phenotypic observations prompted Suchy and others to classify this clinically significant subset of disorders the hepatorenal fibrocystic disorders (HRFD)[19, 20]. Nephronophthisis, Joubert syndrome, Meckel-Gruber syndrome, and Bardet-Biedl syndrome are all examples of HRFD, but the flagship disorder of the HRFD is polycystic kidney disease (PKD).

PKD is a group of heterogeneous single-gene disorders transmitted as either autosomal dominant or autosomal recessive traits. While the formation of fluid-filled cystic structures in the kidney is a common feature, several other key features, including severity of disease, age of onset, and extrarenal manifestations distinguish the dominant and recessive disorders. Autosomal dominant polycystic kidney disease (ADPKD, MIM 173900) is a typically late-onset disorder, with an incidence of 1:1,000. The majority of cases (~85%) results from mutations in *PKD1*, while the remaining ~15% of cases are caused by mutations in *PKD2*[21]. Autosomal recessive polycystic kidney disease (ARPKD, MIM 263200) is less prevalent that ADPKD, with an incidence of 1:20,000 live births. However, though less common, it is a far more severe disorder, typically presenting *in utero* or in the early postnatal period.

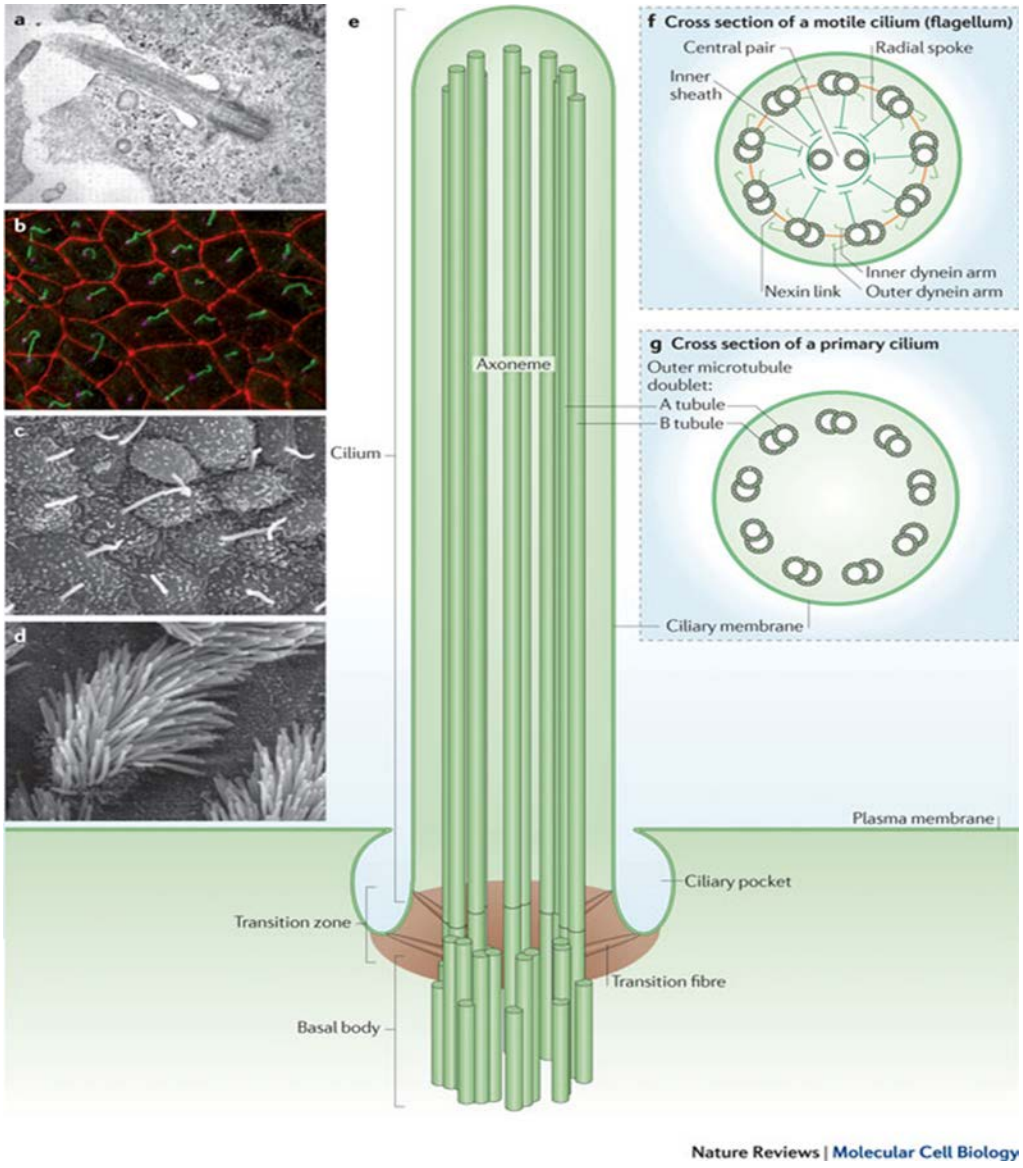

Figure 1.1: The structure of the cilium. A primary cilium of retinal pigment epithelial cells visualized using transmission electron micrograph (A). Immunofluorescence image of primary cilia in inner medullary collecting duct cells showing the cilium (green) anchored to the basal body (magenta) with cell-cell junctions (red) (B). Scanning electron micrographs of mouse nodal cilia (C) and mouse tracheal motile cilia (D). An artistic schema of the structure of the cilium (E). In cross-section schemas, the motile cilium with the central pair of microtubules (F) and the primary, non-motile cilium (G).

Image from "Ciliogenesis: building the cell's antenna"
Nature Reviews Molecular Cell Biology 12, 222-234 (April 2011)
Reprinted with permission from Nature Publishing Group

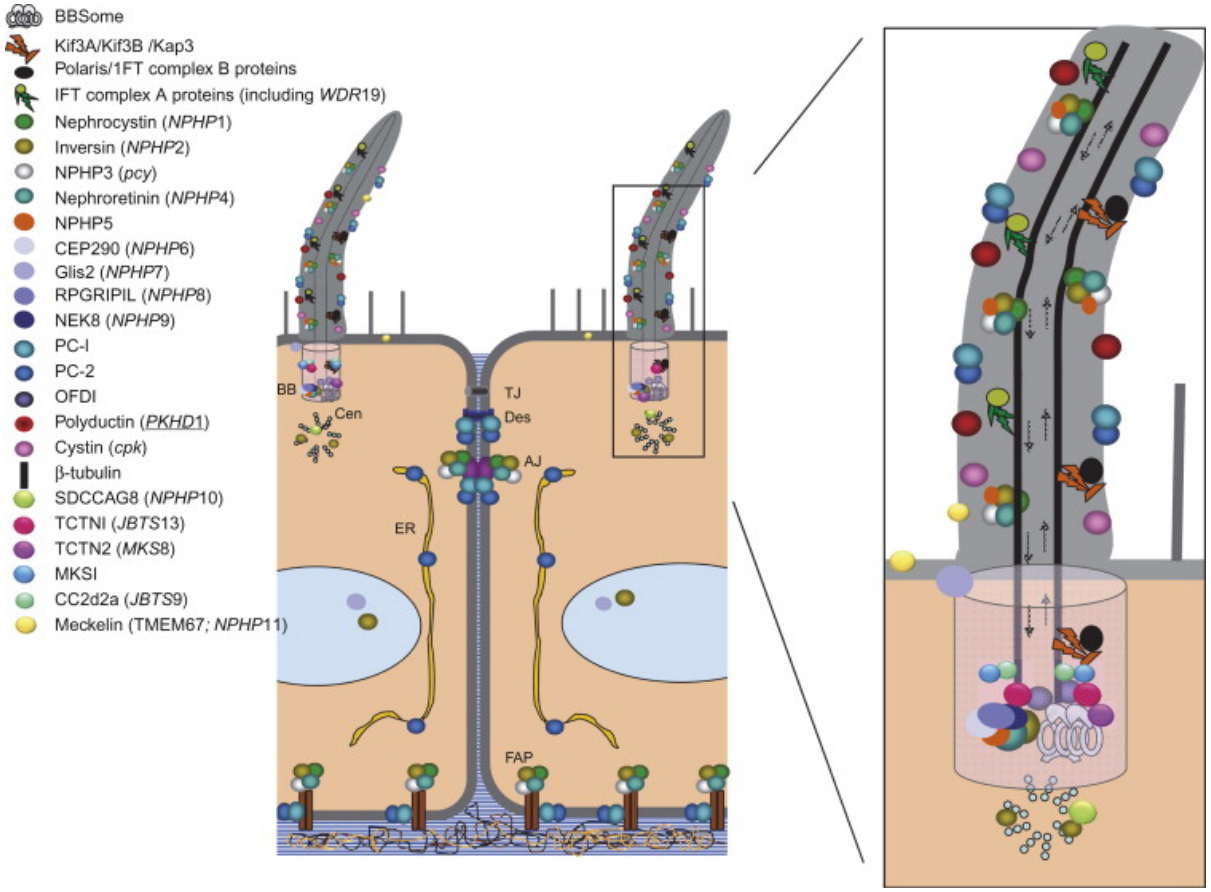

Figure 1.2: The subcellular localization of the cystoproteins.

Image from *Chapter 40: Polycystic Kidney Disease* by Gregory G. Germino and Lisa M. Guay-Woodford in *Chronic Renal Disease*, P. Kimmel and M. Rosenberg, Editors, 2015, Elsevier: San Diego, California, USA
Reprinted with permission from Elsevier Books

Autosomal Recessive Polycystic Kidney Disease

Phenotypic Presentation

ARPKD is a pleiotropic, early onset disorder that presents *in utero* or the early neonatal period with an incidence rate of 1:20,000 live births. However, it is more common in certain populations, *i.e.*, Finnish and Afrikaans [22-24]. It is a leading cause of renal-related morbidity and mortality among children, including end-stage renal disease. The affected patients typically present with bilateral enlarged, echogenic kidneys resulting from the formation of fluid-filled, epithelial-lined cysts in the collecting duct of the nephron, with a loss of corticomedullary differentiation due to medullary hyperechogenicity[25]. Often, affected fetuses present with oligohydramnios, likely a result of poor fetal urine output due to impaired renal function[22, 25]. Oligohydraminos can lead to intrauterine constraint resulting in the "Potter sequence", the syndromic presentation of craniofacial abnormalities, limb defects, and pulmonary hypoplasia, the latter of which is responsible for the estimated perinatal mortality rate of 30%[26, 27]. One-year survival rates of 92-95% have been reported in patients that survive the first month of life[28].

In addition to the renal manifestations, liver involvement invariably occurs in patients with ARPKD, though the severity and clinical presentation varies. The primary lesion involves malformation of the ductal plate, a developmental defect characterized by defective remodeling of the ductal plate with intrahepatic duct dilatation and progressive portal tract fibrosis[29]. Portal tract fibrosis may lead to portal hypertension, hypersplenism, and gastroesophageal varices[28, 30]. The relationship between the severity of the renal and hepatic phenotype in patients with ARPKD defies direct correlation. However,

patients that present with late-onset ARPKD typically have a predominant liver phenotype with either little to no renal involvement[26, 27, 31, 32].

While renal and hepatobiliary structural abnormalities are the key phenotypic features of recessive PKD, a number of other manifestations have been associated with ARPKD. Growth impairment/retardation has been reported in affected children. However the correlation between the proportion of growth impairment and disease severity remains to be established[27, 33, 34]. Systemic hypertension has also been described in children with ARPKD and typically precedes the decrease in glomerular filtration rate. A higher risk of urinary tract infections, particularly in females, has been reported with rates of ~20% to 50% in various cohorts[27, 35-37]. There have also been reports of intracranial aneurisms, though they are very rare[38-40].

Genetics of ARPKD

All typical cases of ARPKD are caused by mutations in a single gene, polycystic kidney and hepatic disease gene 1 (*PKHD1*)[41]. Located on chromosome 6p21.1-p12, *PKHD1* spans over 470-kb of genomic DNA. The transcriptional profile of *PKHD1* is complex; 19 exons have been reported to have alternative splicing boundaries and published data from our laboratory demonstrates that *PKHD1* and its mouse orthologue, *Pkhd1*, undergoes extensively alternative splicing[41, 42]. The longest open reading frame of *PKHD1*, consisting of 67 exons, encodes FPC, a 4059 amino acid, single-pass transmembrane protein predicted to have a long extracellular N-terminus (containing multiple Ig-like, plexin, transcription factor domans (IPT) and parallel beta-helix (PbH1) repeats) and a shorter cytoplasmic C-terminal tail[43, 44]. FPC is has different expres-

sion patterns based on developmental age: during fetal development, FPC is predominantly expressed in the neural tube, early ureteric bud, mesonephric tubules, and immature hepatocytes[45, 46]. In the adult kidney, FPC is primarily expressed in the collecting duct and thick ascending lopes of Henle within the kidney, the bile duct epithelia of the liver, and the pancreas[43, 44, 47, 48].

The function of FPC is unknown, however a number of features of this protein suggest intriguing hypotheses. FPC localizes to the apical primary cilium and basal body in renal tubular cells, along with a number of other cystoproteins[15, 43, 48-52]. Disruptions in many of these proteins or the cilium itself are responsible for the ciliopathies, suggesting that the primary cilium and its protein components serve a central role in the proper development and maintenance of renal tubule structures. The early expression pattern of FPC suggests that perhaps FPC has a role in the early stages of organ development and tubular morphogenesis. Published data has described an interaction between polycystin-1 and polycystin-2, the proteins encoded by the ADPKD disease genes *PKD1* and *PKD2*, respectively[53]. FPC has been shown to interact with polycystin-2, seemingly regulating its expression and function[54]. Indeed, mice with mutations in both *Pkhd1* and either *Pkd1* or *Pkd2*, show a more severe cystic phenotype as compared to mice with a single mutation[54]. Finally, a subset of membrane-bound FPC appears to undergo Notch-like processing resulting in the nuclear localization of the C-terminal tail, and the shedding of the extracellular N-terminal domain into the tubular lumen[55]. The bi-directional release could be part of a signaling cascade required for proper ciliary function. While there are many possible functions of FPC, more directed functional studies

are limited due to the size and transcriptional complexity of FPC, as well as a lack of reliable immunoreagents.

To date, nearly 750 pathogenic mutations in *PKHD1* have been catalogued in the ARPKD Mutation Database (http://www.humgen.rwth-aachen.de), with missense mutations accounting for approximately half of the reported mutations. There is great diversity in the reported ARPKD mutations with pathogenic mutations identified along the full length of the gene. While mutational hotspots are not characteristic of this disease gene, the most common mutation, c.107C>T (p.Thr36Met), accounts for nearly 20% of all mutated alleles. The diversity of mutations in patients with ARPKD makes deciphering a genotype-phenotype correlation very difficult. Indeed, most patients are compound heterozygotes, having inherited a different pathogenic allele from each parent[28, 56]. Despite both the mutational diversity and compound heterogeneity, several phenotypic patterns have been identified. Patients that have inherited two truncating mutations appear to have a more severe disease phenotype, resulting in perinatal mortality[57-61]. However, there are notable exceptions, for example a child who is homozygous for a large PKHD1 deletion surviving well past the neonatal period[62]. While truncating mutations appear to be the most harmful, missense mutations do not always present with a milder phenotype[63]. A number of missense mutations have been described which, when paired with a truncated mutation or in a homozygous form, present with a severe disease phenotype[26, 58, 64].

Mouse Models

Experimental animal models are a mainstay in the study of genetic diseases. However, experimental studies using mouse models of ARPKD are hindered due to the complex molecular profile of *Pkhd1*, the mouse orthologue of the principal human disease gene. Like the human *PKHD1*, *Pkhd1* is an enormous gene and has been shown to have a complicated splicing profile. To date, there have been eight mouse models generated, most using standard gene targeting approaches to produce putative *Pkhd1* null animal, and one model that arose from a truncating mutation in exon 48 (Table 1.1). In addition to these targeted mouse models, the *PCK* rat model, that arose spontaneously in the Crj:CD/SD background due to an exon skipping event involving *Pkhd1* exon 36, resulting in a frame shift mutation[47, 65]. However, these murine models present with a confounding array of phenotypic manifestations that do not accurately phenocopy the human lesion (Table 1.1). While the liver involvement is invariable in all of these animals, the renal disease is highly disparate, particularly in mice, which manifest either no renal involvement or very mild renal disease localized to the proximal tubules instead of the collecting duct. Notably, many of the mouse mutants also present with severe ductal disease of the pancreas. In contrast, clinically significant pancreatic disease is rare in human ARPKD.

The transcriptional complexity of *Pkhd1* may prevent standard gene-targeting strategies from generating a truly null allele. NCBI's ORF Finder (http://www.ncbi.nlm.nih.gov/gorf/gorf.html) suggests that there may be alternative translational start sites (TSS) in *Pkhd1* which, when coupled with the extensive alternative splicing, could result in new transcripts that are capable of generating functional

isoforms[42]. For example, the *Pkhd1*^{tm1Sswi} mouse, which was generated by replacing the first three exons of *Pkhd1* with a *lacZ* reporter, exemplifies the confounding effect that alternative splicing can have on standard gene-targeting approaches. Homozygous *Pkhd1*^{tm1Sswi} mice progressively developed renal cystic disease and were considered to be a *Pkhd1* null based on standard RT-PCR [66]. However, upon further study, Boddu, *et al.* was able to demonstrate the existence of *Pkhd1* amplicons that included exons distal to a putative TSS in exon 37 in the *Pkhd1*^{tm1Sswi} mouse using alternative RT-PCR based strategies[42].

Along with alternative splicing, genetic background also appears to have a significant impact on the severity of the renal lesion in rodents. The *PCK* rat fails to express the renal lesion when the mutation is transferred from the original Sprague-Dawley background onto the Fawn-Hooded background, though the liver phenotype remains unchanged[67]. In addition, the *Pkhd1* del3-4 mouse model showed severe renal disease with high rates of lethality during the initial outbreeding of the founder heterozygotes. However, these phenotypes disappeared upon inbreeding [68]. These studies, which demonstrate an attenuation of disease based on genetic background, suggest that genetic modifiers module the expression of the renal cystic disease phenotype[45].

While disruption of the orthologous *PKHD1* gene in rodents has yet to produce an accurate and reliable experimental model of recessive PKD, at least two non-orthologous models have been reported that do phenocopy the human disease with respect to both the renal and biliary lesions. The BALB/c polycystic kidney (*bpk*) mouse arose from a splicing defect in one of the two isoforms of *Bicc1*, resulting in the partial functional disruption of the RNA-binding protein, bicaudal C[69]. The second model, the congenital pol-

Table 1.1: *Mouse Pkhd1 models*

Type	**Symbol**	**Investigator**	**Mutation**	***Pkhd1*$^{-/-}$**	**Kidney**	**Other**
Targeted Allele	*Pkhd1*^{tm1Rbu}	R. Buettner	Exon 40 skipping	viable	none	Liver*
Targeted Allele	*Pkhd1*^{tm1Cjwa}	C.J. Ward	Exon 2 skipping	viable	PT dilatation	Liver*, Pancreas**
Targeted Allele	*Pkhd1*^{tm1Ggg}	G.G. Germino	Exon 3-4 deletion	PL (29% survive)	TAL and CD	Liver*, Pancreas**
Targeted Allele	*Pkhd1*^{tm1Gwu}	G. Wu	Exon 15-16 deletion	viable	PT and MCD dilatation	Liver*
Targeted Allele	*Pkhd1*^{tm1Som}	S. Somlo	Exon 4 deletion	viable	none	Liver*, Pancreas**
Targeted Allele	*Pkhd1*^{tm1Sswi}	S.S. Williams	Exon 1-3 deletion	viable	PT dilatation	Liver*
Targeted Allele	*Pkhd1*^{tm2Cjwa}	C.J. Ward	Transcription termination intron 2	viable	PT dilatation	Liver*
Spontaneous Allele	*Pkhd1*^{cyli}	L.M. Guay-Woodford	Exon 48 (c.7589delGGinsT)	viable	none	Liver*

Compiled from the Mouse Locus Catalogue http://www.informatics.jax.org/allele/summary?markerId=MGI:2155808

PL = Partial perinatal lethality

PT = Proximal tubule; TAL = Thick ascending limb; CD = Collecting duct; MCD = Medullary collecting duct;

Liver* = Intra-hepatic biliary ductal dysgenesis; Pancreas** = Intra-pancreatic ductal dysgenesis

Reprinted from *Journal of Pediatric Genetics*, 3(2), Guay-Woodford, LM, “Autosomal recessive polycystic kidney disease: the prototype of the hepatorenal fibrocystic diseases” 89–101, 2014, with permission from IOS Press.

ycystic kidney (*cpk*) mouse results from a spontaneous mutation in the *Cys1* gene, which encodes the protein cystin. The *cpk* mouse has become the most extensively character mouse model of ARPKD due to its faithful recapitulation of the human disease phenotypes, however little is known about the molecular function of cystin. It remains to be determined whether cystin and bicaudal C function in a similar molecular pathway with FPC, as the similarities in their disease phenotypes would suggest.

Cystin

Cystin, the protein encoded by *Cys1*, is a 145 amino acid, lipid-raft associated protein primarily expressed in the kidney and liver[70]. Cystin has an N-terminal myristoylation domain, two nuclear localization signals (NLS), and a ciliary localization signal (CLS). The five amino acid CLS, AxEGG, has been validated as a functional motif and is unique to cystin[71]. Cystin colocalizies to the primary cilium along with several other cystoproteins, including FPC[15]. N-terminal myristoylation is thought to be a critical functional component of cystin, having been shown to be necessary but not sufficient for its ciliary localization. Indeed, the CLS works together with myristoylation in ensure proper ciliary localization. The myristoylation domain also works in concert with the polybasic domain to act as a membrane anchor, allowing cystin to associate with the ciliary membrane. When the myristoylation domain is ablated, cystin exhibits increased nuclear localization[71, 72]. Previously published data from our laboratory have demonstrated that the regulated release of cystin from the ciliary membrane is accomplished via a myristoyl-electrostatic switch, a molecular mechanism that has been extensive characterized in the MARCKS proteins[71, 73]. More recently, unpublished data from our la-

boratory suggests that exchange protein directly activated by cAMP (EPAC) phosphorylates cystin at serine 17, causing a change in the overall charge of the polybasic domain, prompting cystin to dissociate from the ciliary membrane and traffic to the nucleus, although the molecular mechanisms that underlie this nuclear localization have yet to be defined.

Expanding on these data, our laboratory recently published a study that provided the first evidence of a nuclear function for cystin. In 2013, Wu *et al.* described and characterized a novel functional protein interaction between cystin and necdin within the nucleus. By interacting with necdin, cystin is able to antagonize the stimulatory effect that necdin has on the P1 promoter of c-Myc, effectively regulating the expression of c-Myc[72]. This finding was particularly significant because elevated c-Myc expression, first described in the *Cys1*$^{cpk/cpk}$ kidneys, has become a hallmark feature of cystic epithelia[51, 66, 74-83]. These data suggest that the cystic phenotype observed in the *cpk* mouse may be due, at least in part, to dysregulation of c-Myc expression.

Purpose of Research

ARPKD is a leading cause of renal-related morbidity and mortality among children, including end-stage renal disease. *Pkhd1*-targeted rodents models have yet to reliably recapitulate the recessive PKD renal phenotype.. Non-orthologous mouse models provide an alternative experimental system, but require more mechanistic investigation before they can be fully utilized. The phenotypic similarities between the *cpk* mouse and human ARPKD suggest that cystin and FPC may function together in the same molecular complex. However, whether there is a direct and/or functional interaction between these

two proteins remains unknown. The hypothesis underlying this project is that cystin, through interactions with its nuclear binding partners, plays a key role in epithelial differentiation; likely through targeted gene regulation facilitated by the interactions between cystin and its nuclear binding partners. Consequently, loss of cystin function results in cystogenesis.

The goals of our studies were to identify and characterize novel interacting partners of myristoylation-deficient cystin and to examine the relationship between cystin and its interacting partners in the context of nuclear import and function(s). The characterization of novel protein interactions will help elucidate the intracellular functions of cystin, thereby providing new insights into the molecular mechanisms responsible for the cystic phenotype observed in the *cpk* mouse, which phenocopies human ARPKD.

Summary of Dissertation

The data presented in this dissertation demonstrate that cystin interacts with nuclear import machinery, providing the first mechanistic evidence for the nuclear import of cystin. In addition, our data implicate cystin in the regulation of the alternative splicing of *Pkhd1*, providing a potential connection between the pathogenesis of the kidney lesion of the *cpk* mouse and human ARPKD. Lastly, the studies herein identify a novel functional interaction between cystin and the ciliary GTPase, Arl3. This functional interaction provides new insights into the intracellular trafficking of cystin, as well as suggesting a mechanistic link between two previously unrelated mouse models of recessive PKD. Together, these data provide further evidence that the *cpk* mouse is an informative model to dissect the pathways involved in the pathogenesis of recessive PKD.

CHAPTER 2

TANDEM AFFINITY PURIFICATION OF CYSTIN, THE CILIARY PROTEIN DISRUPTED IN THE *CPK* MOUSE MODEL OF POLYCYSTIC KIDNEY DISEASE, SUGGESTS ITS ROLE IN SPLICING REGULATION OF *PKHD1*.

by

JACOB A. WATTS, LANDON S. WILSON, TOBY W. HURD, KARA N. ARBOGAST, AMBER K. O'CONNOR, P. DARWIN BELL, AND LISA M. GUAY-WOODFORD

Abstract

Autosomal recessive polycystic kidney disease (ARPKD; MIM 263200), a major renal-related cause of pediatric morbidity and mortality, is caused by mutations in *PKHD1*. Experimental models are a mainstay for studies of human diseases, however, gene-targeting of *Pkhd1* results in mice with little or no kidney disease. In contrast, disruption of the *Cys1* gene in the *cpk* mouse closely phenocopies human ARPKD. Despite the species differences in *PKHD1/Pkhd1* renal disease expression, the phenotypic similarities between the renal lesion in human ARPKD and the *cpk* mouse have prompted us to speculate that the protein products of *Pkhd1* and *Cys1*, fibrocystin/polyductin complex (FPC) and cystin, respectively, function in common molecular pathway(s). The current study was designed to identify cystin-binding partners and the pathways that regulate the intracellular trafficking and nuclear function of cystin. To identify cystin-interacting partners we employed tandem affinity purification (TAP) using mIMCD-3 cells expressing a NSFTAP-cystin construct, which contains a 4.6 kDa tag comprised of two Strep and

one FLAG domain on the N-terminus of a myristoylation-deficient cystin mutant (cystin$_{G2A}$). This mutant form of cystin is unable to stably associate with the membrane and demonstrates enhanced nuclear trafficking. Among the nuclear proteins identified using TAP, direct interactions were found between cystin and the nuclear-entry regulatory proteins, importin α1, α2, and β2. In addition, a number of proteins with splicing-related functions were also identified. Given previous studies in our laboratory that demonstrated *Pkhd1* is transcriptionally complex, we examined the splicing profile of *Pkhd1* using RT-PCR in immortalized collecting duct cell lines isolated from wild type and *Cys1*$^{cpk/cpk}$ kidneys. Our data demonstrate that the splicing profile of *Pkhd1* is altered in the absence of cystin. Taken together, these data indicate that cystin localizes to the nucleus via importin-regulated pathways and our initial observations implicate a role for cystin in the transcriptional regulation of *Pkhd1*. If confirmed by further studies, this would be the first experimental evidence functionally linking cystin and FPC

Introduction

The polycystic kidney diseases (PKD) are single-gene disorders characterized by the development of epithelial-lined cysts in the kidney and liver. PKD is a leading cause of end stage renal disease in both children and adults, and is transmitted as either an autosomal dominant (ADPKD) or autosomal recessive (ARPKD) trait[1]. ADPKD (MIM 173900) affects 1:1,000 individuals, with a majority of cases (85%) being caused by mutations in *PKD1* and the remainder caused by mutations in *PKD2*[2]. ARPKD (MIM 263200) is less frequent, with an incidence rate of 1:20,000 live births[3]. The recessive

form of PKD is caused by mutations in a single gene, *PKHD1*, which encodes the protein fibrocystin/polyductin complex (FPC)[4].

A number of mouse models have been generated with mutations in *Pkhd1*, the mouse orthologue of the human disease gene. However, these orthologous mouse models do not express the typical ARPKD-like phenotype. While the liver involvement is present, the renal disease is either completely absent or mild and late-onset, with cysts forming in the proximal tubules rather than the collecting ducts[5]. A non-orthologous animal model, the congenital polycystic kidney (*cpk*) mouse phenocopies human ARPKD and has become the most extensively characterized mouse model of ARPKD[6]. The *cpk* mouse arose from a spontaneously occurring frame shift mutation in the *Cys1* gene, which encodes the protein product cystin[7]. Cystin, a myristoylated protein, co-localizes within the primary cilium with several other known cystoproteins, including *Pkhd1*[1, 8]. In previous studies, we have demonstrated that cystin associates with the ciliary membrane through lipid-raft microdomains and that this association is regulated by a myristoyl-electrostatic switch mechanism. When cystin is released from the ciliary membrane, it traffics to the nucleus, where it functions as a transcriptional regulator of c-Myc expression[9].

The phenotypic similarities observed between the *cpk* mouse and human ARPKD, resulting from a loss of cystin or disruptions in FPC, respectively, suggests that these proteins may function together in common molecular pathway(s). To date, no direct or functional interaction between cystin and FPC has been identified. Indeed, the intracellular functions of cystin and FPC remain largely undefined, with potential studies of FPC currently limited by its transcriptional complexity and the paucity of robust immunoreagents.

Therefore, we sought to elucidate the functions of cystin by identifying its interacting partners using a modified approach to tandem affinity purification (TAP). This methodology was originally described for identifying protein complexes in yeast, however it was limited by several shortcomings that rendered it inefficient in mammalian cells[10, 11]. The original TAP tag was 21 kDa, and due to its large size, increased the risk of improper protein folding and false interactions. In addition, the original tag contained both a calmodulin binding peptide (CBP) domain and a tobacco etch virus (TEV) protease cleavage site, each presenting unique problems in mammalian cells. Calmodulin is an endogenously expressed protein involved in a number of signaling pathways that will bind to the CBP moiety, resulting in false positive purification results[12]. The TEV domain requires protease cleavage, increasing handling and the likelihood of sample loss or contamination. To obviate these shortcomings, several changes to the tag and protocol were made. The new TAP tag generated by Gloeckner and colleagues, SFTAP, is only 4.6 kDa and consists of two Strep tags and a FLAG tag that can be added to either terminus of the protein of interest[13]. This tag also lacks the CBP moiety, and does not require TEV cleavage, making the protocol more efficient[13, 14].

In order to focus on the interacting partners of cystin that are involved in its intracellular trafficking, as well as to begin elucidating its putative nuclear functions, we used a myristoylation-deficient cystin mutant ($cystin_{G2A}$). This "G2A" mutant lacks the myristoylation site on its N-terminus and is unable to stably associate with lipid-raft microdomains in the ciliary membrane, which results in enhanced trafficking of cystin to the nucleus. In the current study, we used mIMCD-3 cells stably transfected with an N-terminal tagged SFTAP $cystin_{G2A}$ (henceforth referred to as NSFTAP-cystin) as our bait

protein. We were able to successfully purify our bait protein, as well as identify a number of putative cystin interacting partners. Using this data set we validated multiple molecular and physical interactions. Therefore the data presented in this study serves as the foundation for developing a network of cystin-interacting proteins. Analysis of these networks should provide new mechanistic insights into cystin functional pathways related to normal physiological pathways and recessive PKD-related processes. The data presented in this study serves as the foundation for developing a network of protein interactions involving cystin and its role in ARPKD.

Materials and Methods

Solutions:

TBS: 30mM Tris-CL pH 7.4 and 150mM NaCl, stored for up to one month at room temperature. FLAG elution buffer: 200µg/mL FLAG peptide (Sigma-Aldrich, F3290) in TBS stored at -20°C. TAP lysis buffer: 0.5% Nonidet P-40 (Fluka, 74385) and protease inhibitor (Roche, 118361700001) in TBS, made fresh for each use. TAP wash buffer: 0.5% nonidet P-40 in TBS, made fresh for each use. TEN: 50mM Tris pH7.5, 0.5mM EDTA, & 0.3M NaCl) supplemented with 1M DTT, 10mg/mL Lyzozyme, protease inhibitors and 200µL of 10%NP40. MgNaCl: (1.5M NaCl, 12mM MgCl2) PBSGD: (PBS + 10% glycerol + 1mM DTT). Triton X-100 lysis buffer: 150mM NaCl, 50mM Tris-HCl, pH 7.4, 10% glycerol and 1% Triton X100).

Reagents

Microspin columns (GE Healthcare, 27-3565-01), Strep-Tactin Resin (IBA, 2-1206-002), Desthiobiotin elution buffer "10x buffer e" (IBA, 2-1000-025), anti-FLAG M2 agarose (Sigma-Aldrich, A2220), SYPRO-Ruby Stain (Life-Technologies, S12000), and precast SDS-PAGE gels (Life-Technologies, NP0335BOX).

Cell Culture, DNA Constructs, and Transfections

Mouse IMCD-3 cells (ATCC, CRL-2123) were grown in DMEM/F-12 (Life Technologies, 11320-033) with 10% heat-inactivated fetal bovine serum and 1% penicillin/streptomycin. Myristoylation-deficient cystin cDNA[15] was cloned into the NSFTAP vector (generously provided by Dr. Roepman[14]); the empty NSFTAP vector was used as a negative control. To generate the stable NSFTAP cell lines, both constructs were transfected into 90% confluent mIMCD-3 cells using Lipofectamine 2000 (Life-Technologies, 11668027) following the manufacturer's protocol. After 48 hours, the media was replaced with normal culture media supplemented with G418 (Life-Technologies, 11811031 used at 300 μg/mL). Resistant cells were then maintained under G418 (200μg/mL) selection for all subsequent experiments. Full-length Pkhd1 tagged with N-terminal VSV-G and C-terminal V5 in pcDNA 5/FRT/TO (LifeTechnologies) was generously provided by Dr. Feng Qian.

Antibodies

Polyclonal rabbit anti-cystin (70053) described previously[15] and the polyclonal rabbit anti-GFP (Life Technologies, A-11122) were both used at a 1:1000 dilution in 5% milk in PBS + 0.1% Tween20.

TAP Protocol, SDS-PAGE, and In-gel Staining

TAP was preformed per [14], reducing the number of washes to two. Briefly, two 15 cm plates of NSFTAP cells were grown for five-days post confluence and then lysed in the TAP lysis buffer, scraped to collect, and pelleted by centrifugation. The cleared lysate was then incubated with the Strep-Tactin Superflow Resin using end-over-end rotation for 12-18 hours. The lysate was washed twice with TAP wash buffer and then the proteins were eluted from the beads using a desthiobiotin elution buffer. The resulting eluate was then incubated for 3 hours with the anti-FLAG-M2 agarose, followed by two more rounds of washes. Finally, the purified proteins were eluted from the anti-FLAG-M2 resin using a FLAG elution.

The lysate was mixed with the NuPage Sample Buffer and Reducing agent (Life-Technologies, NP0007 & NP0009) per manufacturer's protocol for a final volume of 160µL. The lysate was loaded into a Novex Bis-Tris 4-12% 10-well pre-cast gel (Life-Technologies, NP0335BOX). To accommodate the large volume of lysate, one partition was removed between two wells to make a double-sized well. Following 35 min of electrophoresis at 200V, the gels were briefly washed twice with ddH_20 and then fixed in 40% methanol/10% acetic acid/50% water for 1 hour. The fixative was removed and the

gels were stained in Sypro-Ruby (LifeTechnologies S12000) stain for 12-18 hours (covered, light sensitive). The gels were destained for at least 3 hours in 10% methanol/7% acetic acid, all while continuously being protected from light. Silver staining was done using the SilverQuest staining kit (LifeTechnologies LC6070) following manufacturer's protocol.

In-gel Digestion

SDS gel bands were excised and excess stain was removed by an overnight wash in a 1:1 mixture of 100 mM ammonium bicarbonate and acetonitrile. After destaining, disulfide bonds were reduced by incubation in 25 mM dithiothreitol at 50°C for 30 min. Alkylation of the free thiol groups was carried out with 55 mM iodoacetamide for 30 min protected from light. The gel pieces were washed twice with a 100 mM ammonium bicarbonate for 30 min each and dehydrated in a SpeedVac (Savant) before the addition of the enzyme. Trypsin at 12.5 ng/µl (Promega Gold Mass Spectrometry Grade) was added to each gel sample and incubated overnight at 37°C. Peptides were extracted from the gel pieces by two incubations in a 1:1 mixture of 5% formic acid and 50% aqueous acetonitrile for 15 min each. The extracts were pooled and the buffer evaporated away before the samples were resuspended in 20 µl of 0.1% formic acid prior to MS analysis.

NanocHiPLC-tandem Mass Spectrometry

An aliquot (4 µL) of each digested sample was loaded onto a Nano cHiPLC 200µm x 0.5mm ChromXP C18-CL 3µm 120Å reverse-phase trap cartridge at 2 µL/min

using an Eksigent autosampler. The cartridge was washed for 4 min with 0.1% formic acid in ddH_20. The bound peptides were flushed onto a Nano cHiPLC column 75µm x 15cm ChromXP C18-CL 3µm 120Å with a 90 min linear acetonitrile gradient (5-50%) in 0.1% formic acid at a rate of 300 nl/min using an Eksigent Nano1D+ LC. The column was washed with 90% acetonitrile + 0.1% formic acid for 10 min followed by 5% acetonitrile + 0.1% formic acid for 10 min. The HPLC system and components were purchased from Eksigent in Dublin,CA.

The Applied Biosystems 5600 Triple-Tof mass spectrometer (AB-Sciex, Toronto, Canada) was used to analyze the protein digest. The IonSpray voltage was set to 2300 V and the declustering potential was at 80 V. Ionspray and curtain gases were set at 10 psi and 25 psi, respectively. The interface heater temperature was 120°C. The eluted peptides were subjected to a time-of-flight survey scan from 400-1250 m/z to determine the top twenty most intense ions for MSMS analysis. Product ion time-of-flight scans at 50 msec were carried out to obtain the tandem mass spectra of the selected parent ions over a range from m/z 400-2000. Spectra were centroided and de-isotoped by Analyst software, version TF (Applied Biosystems). A β-galactosidase trypsin digest was used to calibrate the analysis.

In-house MASCOT database searches were carried out using the *Mus musculus* genome from the UniProt database. The mass tolerances for precursor scans and MS/MS scans were set at 0.05 Da. One missed cleavage for trypsin was allowed. A fixed modification of carbamidomethylation was set for cysteine residues; and a variable medication of oxidation was allowed for methionine residues. Proteins with at least one individual peptide MOWSE score of <40 was considered significant.

Generation of recombinant GST-Importin Constructs

GST-Importin α1, GST-Importin α2, and GST-Importin β2 constructs were transformed into One Shot Chemically Competent BL21(DE3) cells (Life Technologies, C6000-03). Cultures were grown to an OD of 0.4-0.6 and protein expression was induced by 0.1 mM IPTG for 4-6 hours. The cells were spun down at 4000g for 10 minutes and the pellet is resuspended in ice cold TEN. The pellet was frozen at -80°C overnight and when thawed 15mL MgNaCl supplemented with 1mg/mL DNAse is added. The lysate was mixed by gentle agitation for several hours at 4°C and finally centrifuged at 20000g for 20 minutes at 4°C, the recombinant protein was confirmed to be present in the cleared lysate.

Immobilizing GST-proteins to beads and GST-pulldown

For each construct, 500-600μL of gluthathione-sepharose slurry (GE Healthcare) is washed three times in cold PBS and spun down at 500g for 2 minutes. The bacterial lysates containing the purified recombinant GST-Importin α1, GST-Importin α2, and GST-Importin β2 constructs are added and incubated at 4°C overnight with gentle agitation. The slurry was then spun down at 500g for 2 minutes at 4°C and washed four times with PBS + 1% TX100 for five minutes. The beads are then washed twice with PBSGD and then resuspended in PBSGD to a 50% slurry and stored at -80°C.

For GST-pulldowns experiments, COS-7 cells (ATCC, CRL-1651) transiently transfected with Cystin-eGFP were lysed Triton X-100 lysis buffer freshly supplemented with both protease and phosphatase inhibitors. After centrifugation, 5μg of the GST-tagged protein beads were added to the lysates and incubated with gentle agitation over-

night at 4°C. The GST-beads were washed, eluted, and subjected to SDS-PAGE analysis.

Pkhd1 RT-PCR

Cells from confluent cultures of wild type and *cpk* mTERT cells were frozen in growth medium (DMEM/F-12 supplemented with 2% FBS, 1% penicillin/streptomycin, 5mL of 100x insulin-transferrin-selenium-G supplement (Simga-Aldrich, i3146), 0.2 mg/mL Dexamethasone (Sigma-Aldrich, D8893-1MG), 20nM 3,3',5-Triiodo-L-thyronine sodium salt (Sigma-Aldrich, T6397-100MG), and 10% DMSO). The generation of the mTERT immortalized wild type collecting duct cells has been previously described[16]. Using the published method, the *cpk* cell lines were mTERT immortalized in the laboratory of Dr. P. Darwin Bell at the Medical University of South Carolina. The RNA was purified using the PerfectPure RNA Tissue Kit (5 Prime #2900317), including the on-column DNase digestion. For RNA isolation, equal cell volumes of wild type and *cpk* mTERT cells were thawed, pelleted, and lysed in 400uL of Lysis buffer + TCEP and purified per the manufacturer's instructions. The RNA was eluted in 100uL of elution buffer and quantified. One microgram of RNA was immediately (never frozen) reverse transcribed into cDNA using the SuperScript III First-Strand Synthesis SuperMix for qRT-PCR kit (Invitrogen #11752) following the manufacturer's instructions. The cDNA was evaluated for genomic contamination using primers in Actin spanning an intron such that cDNA = 400 bp and the gDNA 600 bp (forward: GGAGGGGCCGGACTCATCG-TACTC, Reverse: CCGCATCCTCTTCCTCCCTGGAGAA), and for large transcripts using primers to amplify a 10kb *Prkdc* product (forward: TCAATTCAC-

TGCCTGCCTTCTGGA, reverse: TAACTATGCAACCACTGCACTCGC). For the *Pkhd1* analysis, 1uL of cDNA was used in a 20uL AccuStart Taq DNA Polymerase HiFi PCR reaction (Quanta #95085) with an extension time of 12 minutes per cycle, 35 cycles, and a ramp rate of 1.5˚C/s (DNA Engine Ramp setting on the BioRad C1000 chassis) using *Pkhd1* specific primers for the longest open reading frame (forward: CATTTGAGGCACAAGGCTGACACA, reverse: CTGAGGTCTGGGCGTAACAG). The RT-PCR products were evaluated on a 0.8% agarose in TBE gel including 1X Sybr Safe (Invitrogen S33102) for 35 minutes at 160V.

Results

Overview of TAP protocol

An overview of the protocol used in this study is outlined in Figure 2.1A. Prior to purification, we analyzed the cell lysate for various subcellular markers by western blot, indicating that proteins from the cytoplasm, membrane, and nucleus were released during cell lysis and are represented in the lysate (data not shown).

Cystin is purified and retained through TAP protocol

To assess the efficacy of the purification, samples from each step of the protocol were subjected to SDS-PAGE for in-gel staining. As shown in Figure 2.1B (upper panel), the TAP protocol substantially reduces the complexity of the protein profile of the starting lysate. Silver staining was initially used for visualization of the proteins (Figure 2.1B, upper panel). However, silver staining has been shown to negatively impact downstream MS analysis by modifying lysine resides within proteins and preventing proper

trypsin digestion[17, 18]. To circumvent this issue, we stained our samples with SYPRO Ruby, which has similar sensitivity to silver staining and does not alter protein resides or interfere with MS analysis (Figure 2.1B, upper panel, far right lane)[19].

To confirm that our bait protein, NSFTAP-cystin, was purified and enriched using TAP, samples retained from each step of the purification process were subject to immunoblotting. Using an anti-cystin antibody, we show that NSFTAP-cystin was present in the whole cell lysate, in each intermediate elution, and in the final elution (Figure 2.1B, lower panel, arrowhead). Importantly, NSFTAP-cystin was absent from the washes, underscoring the efficiency of the protocol. Taken together, these data show that the TAP protocol purified NSFTAP-cystin, while reducing the protein profile of the initial lysate.

Classification of purified proteins

To test the efficacy and reproducibility of this protocol in isolating potential interacting partners of cystin$_{G2A}$, we performed the protocol four times. Using NSFTAP-cystin, the collective dataset of all four experimental MS runs contained 549 individual proteins, of which 110 (19%) were found three or more times (Figure 2.2A). To determine whether our experimental dataset contained false positives, a negative control cell line expressing the empty TAP vector (without cystin) was subjected to the same purification protocol. Following MS analysis, any proteins found in either the negative control dataset, or a reference list of common "sticky proteins" (http://www.dkfz.de/gpcf/251.html) were classified as false positives and excluded from subsequent analysis.

The subcellular locations and functions, as defined by Uniprot (http://www.uniprot.org/) and Ingenuity IPA (http://www.ingenuity.com/products/ipa), were used to further classify the 110 proteins. These proteins are associated with various subcellular compartments, including the cytoplasm, cilium, nucleus, and mitochondria (Figure 2.2B). Interestingly, the proteins belong to a variety of functional categories; a number of which are shown to have a nuclear role, signifying that our NSFTAP-cystin dataset was enriched for nuclear interacting partners (Figure 2.2C)[9].

Putative nuclear interactome of cystin

The overexpression of c-Myc was first described in the kidneys of *cpk* mice and has become a hallmark feature of cystic epithelia[20]. Our laboratory has previously demonstrated that cystin traffics to the nucleus and regulates c-Myc expression through its interaction with necdin[9]. To further assess the nuclear functions of cystin, we generated a string map of the putative interacting nuclear proteins identified with our TAP protocol using STRING (http://www.string-db.org), a web-based application designed to visualize both known and predicted protein-protein interactions (Figure 2.3). The putative cystin-interacting network offers insights into potential nuclear function(s) of cystin by identifying the molecular complexes within the nucleus with which cystin interacts.

Cystin directly interacts with various importin subunits

The regulatory mechanism by which cystin is trafficked to and subsequently enters the nucleus remains unknown. Previously published analysis of cystin described two nuclear localization signals (NLS); however only one appears to be functional[15]. In the

classic mechanism, active transport into the nucleus is regulated by an importin α:β heterodimer. In this mechanism, importin α acts as an adaptor protein, interacting with the NLS of the cargo protein and subsequently complexing with the β subunit which then carries the cargo across the nuclear pore complex[21]. Several importin subunits, both α and β, were found in our TAP dataset, suggesting they may play a role in regulating the nuclear import of cystin.

To validate these cystin-importin interactions, we used a GST-pulldown approach with GST-Importin α1, GST-Importin α2, or GST-Importin β2. Lysates from COS-7 cells that had been transiently transfected with cystin::eGFP were incubated with the immobilized recombinant GST proteins. As shown in Figure 2.4, direct interactions were observed between cystin and Importin α1, α2, and β2. These data provide the first mechanistic evidence for a cystin nuclear entry pathway.

Cystin is implicated in the transcriptional regulation of Pkhd1 splicing

Nearly 25% of the nuclear proteins identified by TAP have been linked to splicing-related functions (Figure 2.3, green nodes; Table 2.1). This finding is noteworthy because our laboratory has previously shown that *Pkhd1*, the mouse orthologue of the disease gene involved in human ARPKD, is transcriptional complex[22]. In our original study, the splicing profile of *Pkhd1* was evaluated using whole kidneys from age and gender matched wild type mice. However, the renal lesion in recessive PKD primarily involves the collecting ducts. Thus, to specifically evaluate the splicing profile of *Pkhd1* as it pertains to recessive PKD, we repeated these studies using immortalized collecting

duct cell lines harvested from wild type and *Cys1*$^{cpk/cpk}$ mice (henceforth referred to as wild type and *cpk* mTERT cells, respectively)[16].

Using primers to the longest open reading frame of *Pkhd1*, RT-PCR was performed on the wild type and *cpk* mTERT cells. As shown in Figure 2.5, the splicing profile of *Pkhd1* is altered in the absence of cystin when compared to the wild type control. These initial data implicate a role for cystin in the regulation of *Pkhd1* splicing and suggest that perturbations in the *Pkhd1* splicing profile may contribute to the cystic phenotype observed in the *cpk* mouse.

Discussion

TAP is a powerful proteomic tool that can aid in elucidating the functions of proteins through their associations with other proteins in molecular complexes. In this study, we sought to define the nuclear functions of cystin. Therefore, we performed TAP on a myristoylation-deficient cystin, which we have previously shown to have enhanced nuclear localization. This construct serves as a useful tool to identify the molecular complexes with which cystin interacts within the nucleus, including those involved in nuclear trafficking and transcriptional regulation. The interaction map generated from our dataset reveals novel insights into cellular processes and pathways in which cystin may participate.

In the classical model of nuclear import, the importin heterodimer, consisting of a α and β subunit, regulates the entry of the proteins into the nucleus through the nuclear pore complex (NPC). The α subunit binds to the cargo protein while the β subunit binds the α and moves the complex across the NPC. This form of active nuclear transport is

energy dependent, requiring the hydrolysis of GTP, by the GTPase Ran, to stimulate the release of the cargo protein from the importin heterodimer once inside the nucleus[23]. However, active transport via the importin heterodimer is not the only method of nuclear entry. Small particles under 40 kDa can passively diffuse through the NPC[24].

Our studies using the myristoylation-deficient cystin construct with enhanced nuclear localization, identified putative interactions between $cystin_{G2A}$ and multiple importin subunits. The purification of these importin subunits, along with Ran, suggests this interaction is likely due to the active transport of cystin into the nucleus. Supporting this hypothesis, direct interactions between cystin and the importin α subunits were confirmed using GST-pulldowns. These data suggest that cystin is actively transported across the NPC through an importin-regulated process, despite its diffusion permissive molecular size (<40 kDa).

Interestingly, we also confirmed a direct interaction between cystin and importin β-2. Previously published data have demonstrated that importin β-2 regulates the ciliary entry of several proteins, specifically the kinesin-2 motor KIF17 and retinitis pigmentosa 2[25, 26]. Direct interaction between cystin and importin β-2 suggests that importin β-2 may be responsible for regulating the entry of the cystin into the cilium. While it is tantalizing to speculate that the cystin-importin β-2 interaction is involved in regulated entry to both the nucleus and the cilium, further studies are required to establish these putative mechanisms.

Approximately 25% of the nuclear proteins identified in our study are functionally associated with splicing, suggesting that cystin may have a role in this nuclear mechanism. Previously published data from our laboratory demonstrates that *Pkhd1*, the mouse

orthologue of the human ARPKD disease gene, undergoes extensive alternative splicing, and the generation of alternative transcripts may be linked to the pathogenesis of recessive PKD[22]. Therefore, we evaluated the splicing profile of *Pkhd1* in immortalized collecting duct cell lines, ***i.e.*** wild type and *cpk* mTERT cells. Using the approach described by Boddu *et al.*, we demonstrate that the *Pkhd1* splicing pattern is indeed different in the *cpk* mTERT cells when compared to wild type control cells. These data suggest that the cystic phenotype observed in the *cpk* mouse may be the cumulative result of several additive factors, ***e.g.,*** dysregulation of c-Myc expression and perturbations in *Pkhd1* splicing, which both arise from a loss of cystin.

While the altered splicing profile of *Pkhd1* in the *cpk* mTERT cells is intriguing, further analysis is required to validate this finding. The amplicons observed in Figure 2.5 must be subcloned and sequenced to ensure that they are indeed *Pkhd1* and not an artifact of the PCR. In order to verify the authenticity of these amplicons, we will follow the approach used by Boddu, ***et al.*** Briefly, the bands will be excised from the gel, subcloned, and subjected to restriction enzyme fingerprinting, an essential process, as each amplicon likely represents more than one transcript. Subsequently the subclones will be grouped based on the results of the restriction enzyme fingerprinting and a representative subclone from each grouping will sequenced to ensure that the amplicons are *Pkhd1* products that are in-frame with the longest open reading frame of *Pkhd1*.

Exons contain splice enhancer (ESE), motifs that are bound by regulatory factors, such as the serine/arginine rich splicing factor (SRSF) family of proteins, to facilitate splicesome/mRNA interactions[27]. Boddu, ***et al.*** made a critical observation about the role of SRSF proteins in *Pkhd1* splicing, specifically SRSF5. This study demonstrated

that ablation of the SRSF5 binding motif in exon 51 caused exon skipping, resulting in a putative frameshift and protein truncation[22]. This observation suggests that SRSF proteins play a critical role in the regulation of alternative splicing.

While none of the SRSF proteins were purified using our TAP protocol, STRING analysis shows that 7 of 13 splicing-related proteins in our nuclear interactome (Table 2.1) directly interact with SRSF5 (data not shown). Therefore, we speculate that cystin may function as part of a molecular complex that involves the SRSF proteins, as well as other splicing-related proteins found in our nuclear interactome (Figure 2.3, green nodes; Table 2.1). Loss of cystin, such as in the *cpk* mouse, may disrupt splicing regulatory machinery, either with respect to stability or function, thereby resulting in the altered splicing profile of *Pkhd1* observed in the *cpk* mTERT cells.

The data presented in this study provide new and provocative insights into the molecular functions of cystin, including mechanisms that regulate its nuclear and perhaps ciliary trafficking, as well as its potential role in regulating the transcription profile of genes, like *Pkhd1*, that undergo extensive alternative splicing. Perhaps most importantly, these data offer the first insights linking *Cys1* and *Pkhd1* in a common pathway and provide a rationale for an expanded study of the role that cystin plays in splicing regulation, particularly of *Pkhd1*.

Acknowledgments

The authors would like to thank Jingyu Guo, Ph.D. for his invaluable guidance in constructing the interaction map.

References

1. Somlo, S., Guay-Woodford L., *Genetic Diseases of the Kidney*. First ed2009: Elsevier.
2. Rossetti, S., et al., *Comprehensive molecular diagnostics in autosomal dominant polycystic kidney disease.* J Am Soc Nephrol, 2007. **18**(7): p. 2143-60.
3. Guay-Woodford, L.M. and R.A. Desmond, *Autosomal recessive polycystic kidney disease: the clinical experience in North America.* Pediatrics, 2003. **111**(5 Pt 1): p. 1072-80.
4. Harris, P.C. and S. Rossetti, *Molecular genetics of autosomal recessive polycystic kidney disease.* Mol Genet Metab, 2004. **81**(2): p. 75-85.
5. Guay-Woodford, L.M., *Autosomal recessive polycystic kidney disease: the prototype of the hepato-renal fibrocystic diseases.* J Pediatr Genet, 2014. **3**(2): p. 89-101.
6. Guay-Woodford, L., *Murine models of polycystic kidney disease: molecular and therapeutic insights.* Am J Physiol Renal Physiol, 2003. **285**(6): p. F1034-49.
7. Hou, X., et al., *Cystin, a novel cilia-associated protein, is disrupted in the cpk mouse model of polycystic kidney disease.* J Clin Invest, 2002. **109**(4): p. 533-40.
8. Yoder, B., X. Hou, and L. Guay-Woodford, *The polycystic kidney disease proteins, polycystin-1, polycystin-2, polaris, and cystin, are co-localized in renal cilia.* J Am Soc Nephrol, 2002. **13**(10): p. 2508-16.
9. Wu, M., et al., *The ciliary protein cystin forms a regulatory complex with necdin to modulate Myc expression.* PLoS One, 2013. **8**(12): p. e83062.
10. Puig, O., et al., *The tandem affinity purification (TAP) method: a general procedure of protein complex purification.* Methods, 2001. **24**(3): p. 218-29.
11. Gavin, A.C., et al., *Functional organization of the yeast proteome by systematic analysis of protein complexes.* Nature, 2002. **415**(6868): p. 141-7.
12. Agell, N., et al., *Modulation of the Ras/Raf/MEK/ERK pathway by Ca(2+), and calmodulin.* Cell Signal, 2002. **14**(8): p. 649-54.
13. Gloeckner, C.J., et al., *A novel tandem affinity purification strategy for the efficient isolation and characterisation of native protein complexes.* Proteomics, 2007. **7**(23): p. 4228-34.
14. Gloeckner, C., K. Boldt, and M. Ueffing, *Strep/FLAG tandem affinity purification (SF-TAP) to study protein interactions.* Curr Protoc Protein Sci, 2009. **Chapter 19**: p. Unit19.20.
15. Tao, B., et al., *Cystin localizes to primary cilia via membrane microdomains and a targeting motif.* J Am Soc Nephrol, 2009. **20**(12): p. 2570-80.
16. Steele, S.L., et al., *Telomerase immortalization of principal cells from mouse collecting duct.* Am J Physiol Renal Physiol, 2010. **299**(6): p. F1507-14.
17. Gevaert, K. and J. Vandekerckhove, *Protein identification methods in proteomics.* Electrophoresis, 2000. **21**(6): p. 1145-54.
18. Rabilloud, T., *Mechanisms of protein silver staining in polyacrylamide gels: a 10-year synthesis.* Electrophoresis, 1990. **11**(10): p. 785-94.
19. Lopez, M.F., et al., *A comparison of silver stain and SYPRO Ruby Protein Gel Stain with respect to protein detection in two-dimensional gels and identification by peptide mass profiling.* Electrophoresis, 2000. **21**(17): p. 3673-83.

20. Cowley, B.J., et al., *Elevated proto-oncogene expression in polycystic kidneys of the C57BL/6J (cpk) mouse.* J Am Soc Nephrol, 1991. **1**(8): p. 1048-53.
21. Stewart, M., *Molecular mechanism of the nuclear protein import cycle.* Nat Rev Mol Cell Biol, 2007. **8**(3): p. 195-208.
22. Boddu, R., et al., *Intragenic motifs regulate the transcriptional complexity of Pkhd1/PKHD1.* J Mol Med (Berl), 2014. **92**(10): p. 1045-56.
23. Fried, H. and U. Kutay, *Nucleocytoplasmic transport: taking an inventory.* Cell Mol Life Sci, 2003. **60**(8): p. 1659-88.
24. Rodriguez, M.S., C. Dargemont, and F. Stutz, *Nuclear export of RNA.* Biol Cell, 2004. **96**(8): p. 639-55.
25. Dishinger, J.F., et al., *Ciliary entry of the kinesin-2 motor KIF17 is regulated by importin-beta2 and RanGTP.* Nat Cell Biol, 2010. **12**(7): p. 703-10.
26. Hurd, T.W., S. Fan, and B.L. Margolis, *Localization of retinitis pigmentosa 2 to cilia is regulated by Importin beta2.* J Cell Sci, 2011. **124**(Pt 5): p. 718-26.
27. Lin, S. and X.D. Fu, *SR proteins and related factors in alternative splicing.* Adv Exp Med Biol, 2007. **623**: p. 107-22.

Table 2.1: *Proteins involved in splicing identified by TAP*

Gene	Protein	Function
Ddx5	DDX5	Alternative regulation of pre-mRNA splicing
Dx39a	DDX39A	Involved in pre-mRNA splicing; required for the export of mRNA from the nucleus
Hspa8	HSPA8	Component of the PRP19 complex, an integral part of the spliceosome
Nono	NONO	Involved in pre-mRNA splicing, probably as a heterodimer SFPQ
Prp19	Pre-mRNA Processing F19	Involved in the assembly of the spliceosome
Prp31	Pre-mRNA Processing F31	Involved in pre-mRNA splicing, integral part of the spliceosome
Sf3a1	Splicing Factor 3A S1	Subunit of splicing factor 3A
Sf3a3	Splicing Factor 3A S3	Subunit of splicing factor 3A
Sf3b3	Splicing Factor 3B S1	Subunit of splicing factor 3B
Sfpq	SF P/Q-Rich	Essential pre-mRNA splicing factor; required in early spliceosome assembly
Snrpa	U2 snRNP A	Essential of recognition of pre-mRNA 5' splice-site and spliceosome assembly.
Snrpd2	SM-D2	Core component of the U1, U2, U4, & U5 snRNPs, building blocks of the spliceosome
Snrpd3	SM-D3	Core component of the U1, U2, U4, & U5 snRNPs, building blocks of the spliceosome

Protein functions from Uniprot (http://www.uniprot.org/)

Figure 2.1: Tandem affinity purification with NSFTAP-cystin. (A) Overview of TAP protocol. (B) Samples from the indicated steps of the protocol were assessed by in-gel staining. Upper panel: silver staining shows a progressive decrease in the total number of proteins in each successive step of the purification. The final elution reveals distinct bands. For mass spectrometry SYPRO Ruby was used to visualize the proteins (far right lane). Lower panel: immunoblot analysis using anti-cystin antibodies shows that the tagged cystin (upper band arrowhead) was purified and enriched throughout the protocol. The lower band is endogenous cystin.

Figure 2.2: Classification of the proteins purified with NSFTAP-cystin. (A) A total of 549 individual proteins were identified, with 110 proteins identified in 3 or more runs. (B) The 110 proteins originate from a variety of subcellular locations and belong to a number of different functional categories (C).

Figure 2.3: Putative interaction network of the cystin-interacting nuclear proteins. This map contains all of the proteins classified as nuclear proteins by Uniprot. Cystin is indicated in blue, the various importin proteins are shown in orange, and proteins with splicing-related functions are highlighted in green.

Figure 2.4: Validation of protein interactions. GST-pulldown experiments were performed to test for interactions between cystin and several of the importin proteins identified by TAP, confirming interactions between cystin and importin β-2, importin α-1, and

importin α-2. Retinitis pigmentosa 2 is used as a positive control for GST-pull down experiments based on previously published data[26].

Figure 2.5: Comparative *Pkhd1* transcriptome in wild type and *cpk* mTERT cells. A splicing profile of *Pkhd1* in wild type and *cpk* mTERT cells was generated by RT-PCR using primers for the longest open reading frame. The *Pkhd1* profile differs in the *cpk* mTERT cells compared to the wild type control, with the absence of several amplicons (red arrows) and as well as the appearance of new amplicons (blue arrows). The longest open reading frame of Pkhd1 was amplified by PCR using exon specific primers for exons 1 and 67. The figure represents n=3 experiments.

Figure 2.1

A

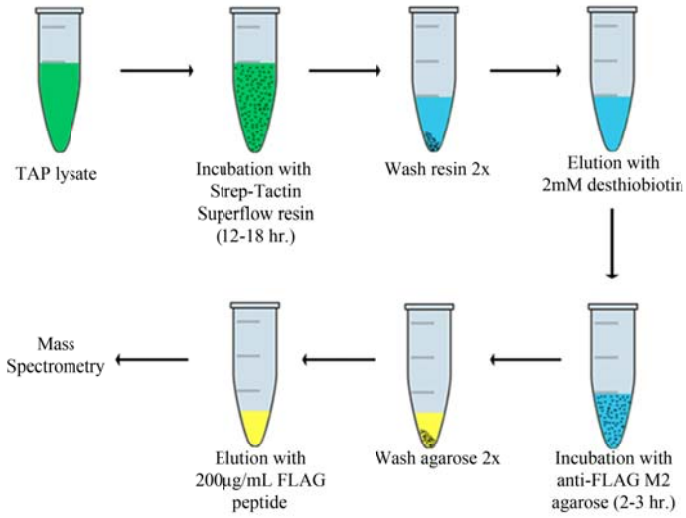
TAP lysate
Incubation with Strep-Tactin Superflow resin (12-18 hr.)
Wash resin 2x
Elution with 2mM desthiobiotin
Incubation with anti-FLAG M2 agarose (2-3 hr.)
Wash agarose 2x
Elution with 200µg/mL FLAG peptide
Mass Spectrometry

B

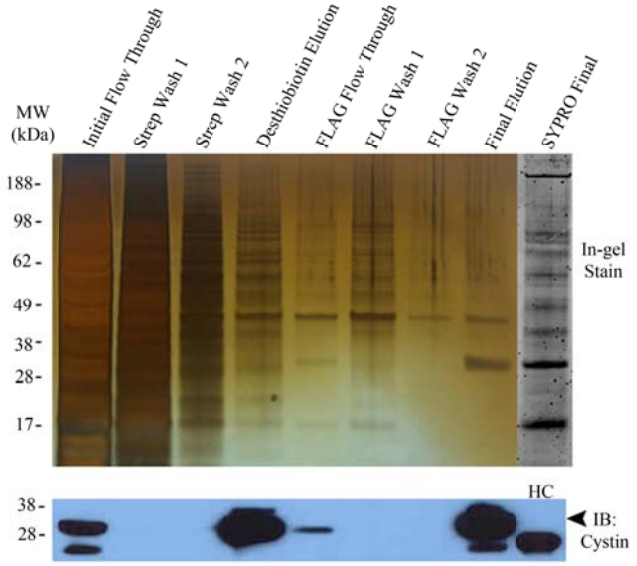
MW (kDa)
Initial Flow Through
Strep Wash 1
Strep Wash 2
Desthiobiotin Elution
FLAG Flow Through
FLAG Wash 1
FLAG Wash 2
Final Elution
SYPRO Final
188-
98-
62-
49-
38-
28-
17-
In-gel Stain
HC
38-
28-
IB: Cystin

Figure 2.2

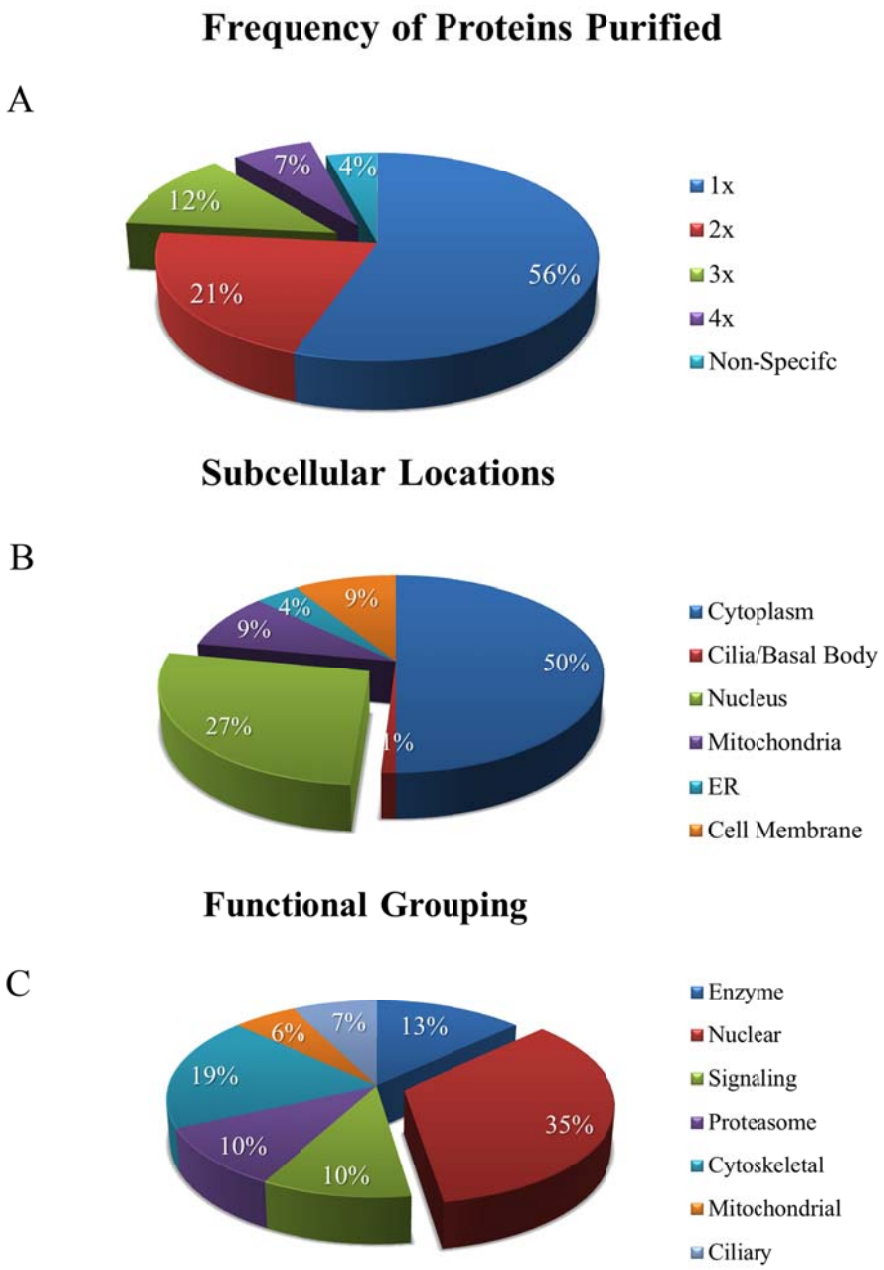
Frequency of Proteins Purified
A
7%
4%
12%
21%
56%
1x
2x
3x
4x
Non-Specifc
Subcellular Locations
B
9%
4%
9%
50%
27%
1%
Cytoplasm
Cilia/Basal Body
Nucleus
Mitochondria
ER
Cell Membrane
Functional Grouping
C
7%
13%
6%
19%
35%
10%
10%
Enzyme
Nuclear
Signaling
Proteasome
Cytoskeletal
Mitochondrial
Ciliary

Figure 2.3

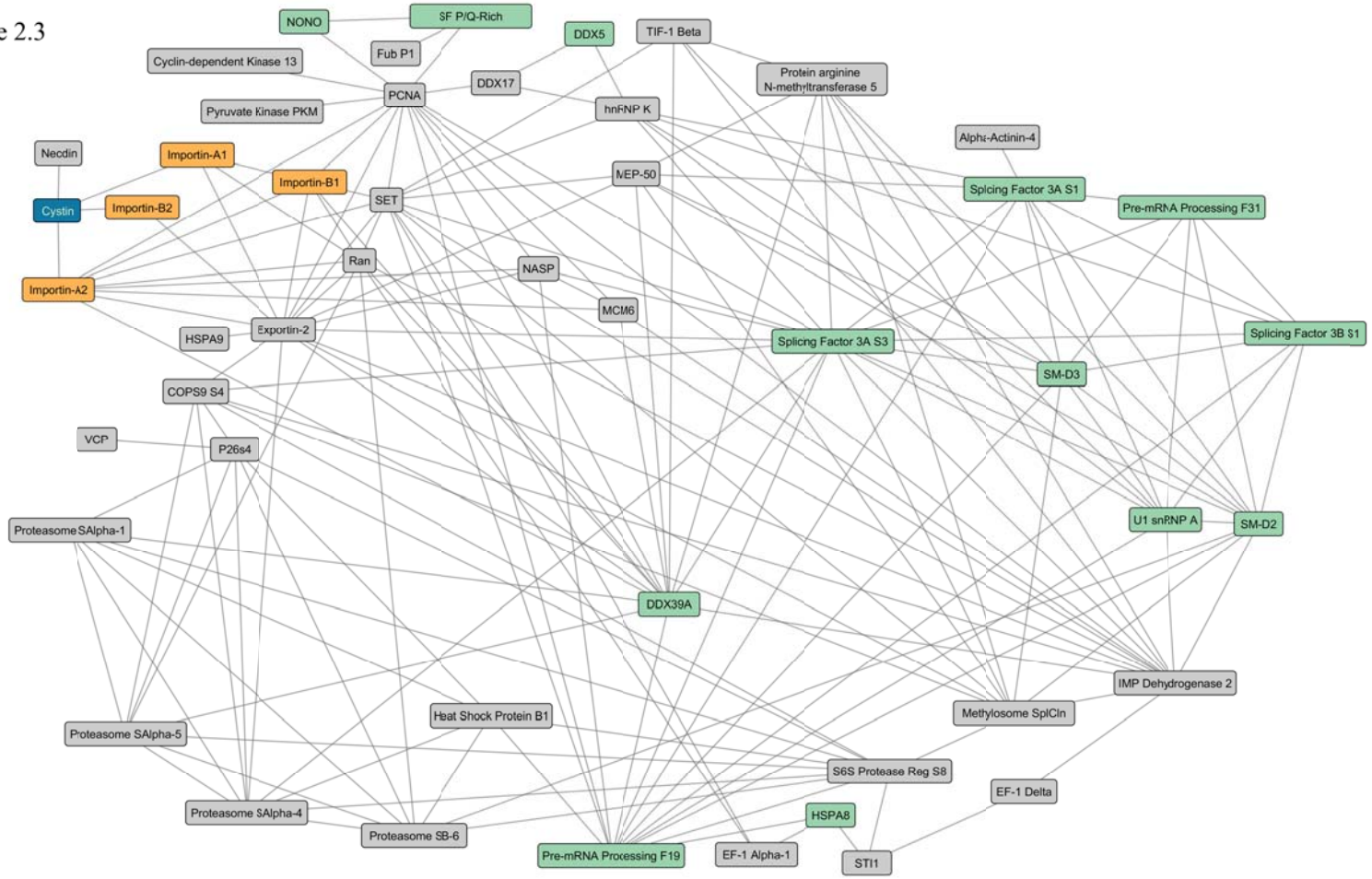
NONO
SF P/Q-Rich
DDX5
TIF-1 Beta
Fub P1
Cyclin-dependent Kinase 13
DDX17
Protein arginine N-methyltransferase 5
PCNA
Pyruvate Kinase PKM
hnRNP K
Alpha-Actinin-4
Necdin
Importin-A1
Importin-B1
MEP-50
Splicing Factor 3A S1
Cystin
Importin-B2
SET
Pre-mRNA Processing F31
Ran
NASP
Importin-A2
MCM6
HSPA9
Exportin-2
Splicing Factor 3A S3
Splicing Factor 3B S1
SM-D3
COPS9 S4
VCP
P26s4
U1 snRNP A
SM-D2
Proteasome SAlpha-1
DDX39A
IMP Dehydrogenase 2
Heat Shock Protein B1
Methylosome SpICln
Proteasome SAlpha-5
S6S Protease Reg S8
EF-1 Delta
Proteasome SAlpha-4
HSPA8
Proteasome SB-6
Pre-mRNA Processing F19
EF-1 Alpha-1
STI1

Figure 2.4

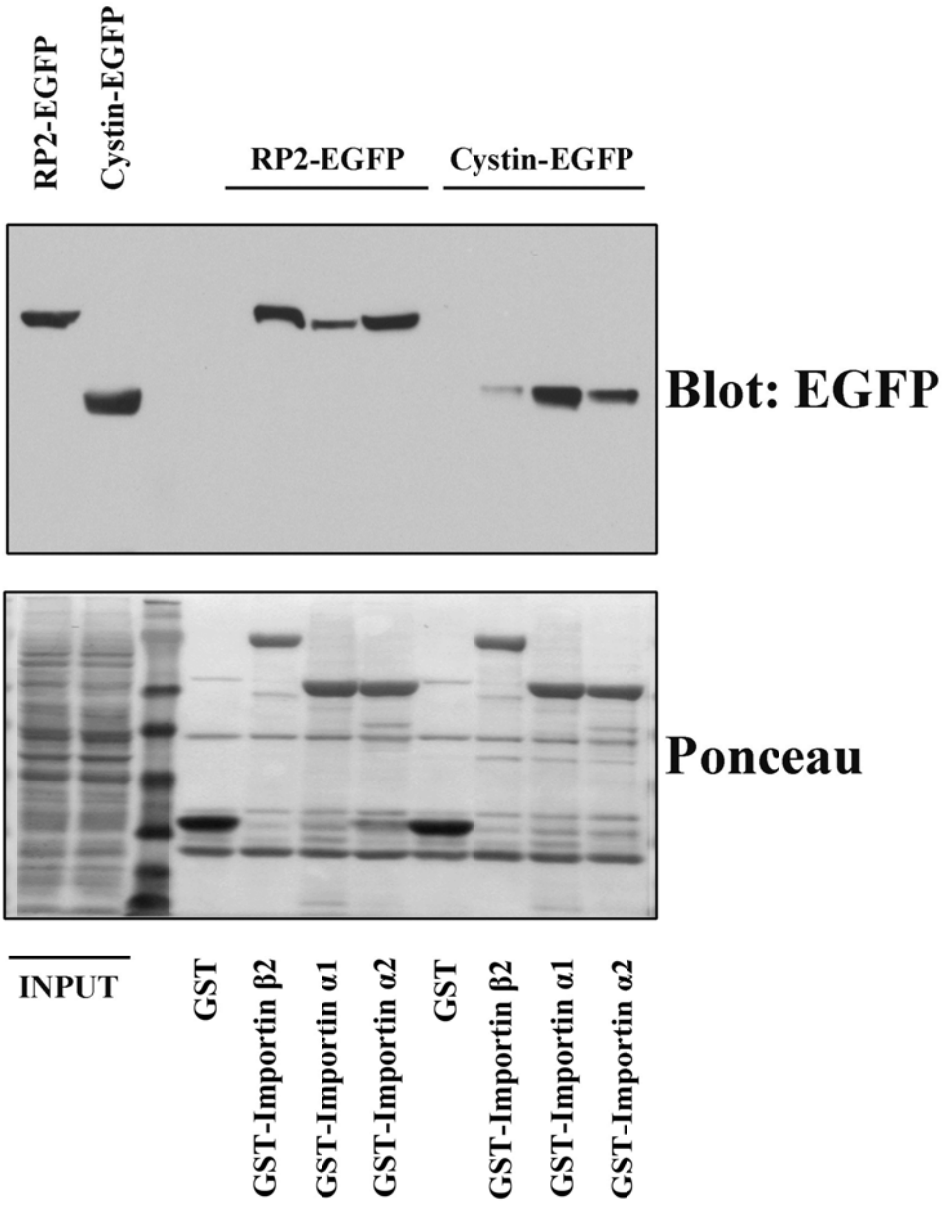
RP2-EGFP
Cystin-EGFP
RP2-EGFP
Cystin-EGFP
Blot: EGFP
Ponceau
INPUT
GST
GST-Importin β2
GST-Importin α1
GST-Importin α2
GST
GST-Importin β2
GST-Importin α1
GST-Importin α2

Figure 2.5

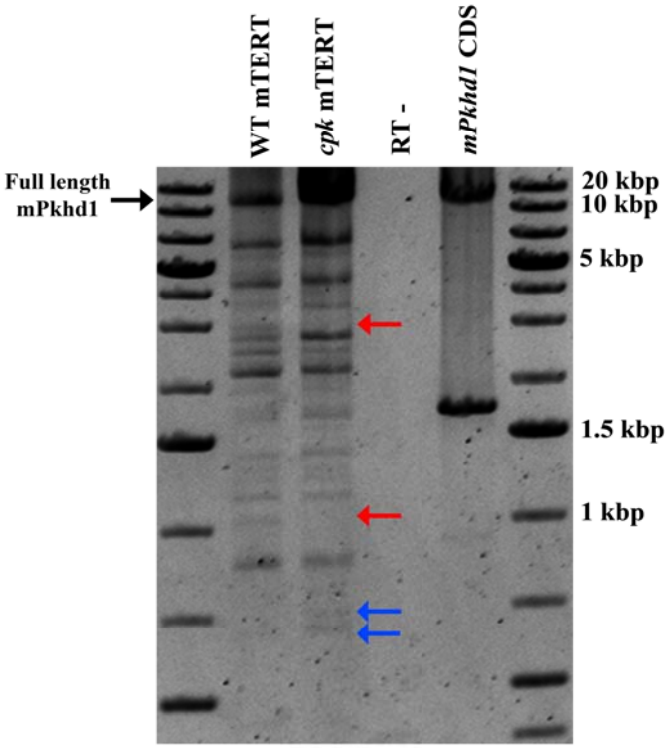
WT mTERT
cpk mTERT
RT -
mPkhd1 CDS
Full length mPkhd1
20 kbp
10 kbp
5 kbp
1.5 kbp
1 kbp

CHAPTER 3

CRISPR-MEDIATED KNOCKDOWN OF ARL3 REVEALS A FUNCTIONAL INTERACTION WITH CYSTIN, THE CILIARY PROTEIN DISRUPTED IN THE *CPK* MOUSE MODEL OF RECESSIVE POLYCYSTIC KIDNEY DISEASE

by

JACOB A. WATTS, P. DARWIN BELL, AND LISA M. GUAY-WOODFORD

Abstract:

Autosomal recessive polycystic kidney disease (ARPKD; MIM 263200) is a leading cause of pediatric morbidity and mortality. The *cpk* mouse, which arose spontaneously from a frameshift mutation in *Cys1*, phenocopies human ARPKD and is established as the best characterized mouse model of recessive PKD. We have previously shown that cystin, the protein product of *Cys1*, regulates the expression of c-Myc through its nuclear interaction with necdin. Using tandem affinity purification strategies, we have identified the ciliary GTPase, Arl3, as a putative cystin interacting partner. Arl3 has been shown to regulate the ciliary localization of myristoylated proteins, specifically cystin, and *Arl3*$^{-/-}$ mice present with a renal cystic phenotype similar to that observed in the *cpk* mouse. In the current study, we used CRISPR technology *in vitro* to knockdown Arl3 expression (Arl3^{CRISPR}) to investigate the interactions between cystin and Arl3. Increased expression of c-Myc, a hallmark feature of cystic epithelia, was used as a molecular biomarker. Our data suggest that the cystic phenotype observed in the Arl3$^{-/-}$ mouse may be due to disruption in the association of cystin with lipid microdomains in the ciliary membrane.

These findings suggest that cystin and Arl3 are involved in a molecular complex required to maintain normal ciliary signaling and renal epithelial homeostasis and that loss of either protein results in cystogenesis.

Introduction

Primary cilia are small, thin, membrane-bound organelles that originate from the basal body and protrude from the apical plasma membrane of the cell. They are essential for the proper physiological regulation of a number of cellular and developmental processes, *e.g.,* Hedgehog and WNT signaling, as well as left-right patterning and limb development. Disruptions in either the structure or function of the primary cilium results in the onset and progression of a number of diseases, broadly classified as ciliopathies[1-3]. Hepatorenal fibrocystic diseases, a clinically important subset of ciliopathies, are diseases that present with fibrocystic disease in the kidney and liver, including Nephronophthisis, Bardet-Biedl syndrome, and Polycystic Kidney Disease[4-6].

Autosomal recessive polycystic kidney disease (ARPKD; MIM 263200) is an inherited, monogenic disorder characterized by the formation of cysts arising from ductal structures in the kidney and liver. In humans, ARPKD occurs due to mutations in the *PKHD1* gene[7, 8]. ARPKD typically presents *in utero* or in the early post-natal period, with an incidence of 1:20000 live births, and is a major renal-related cause of morbidity and mortality in infants and children[9].

In an effort to understand the molecular mechanisms that underlie the pathogenesis of ARPKD, at least eight mouse models have been generated with a variety of targeted mutations in *Pkhd1*, the mouse orthologue of the human disease gene. The result-

ant mice, however, are phenotypically distinct and do not accurately phenocopy the severe disease phenotype observed in human ARPKD[10]. While the ARPKD-like liver phenotype in these mice is invariably present, the renal lesion is either absent or mild, with cystogenesis involving the proximal tubules instead of the collecting ducts.

Although an orthologous mouse model that phenocopies human ARPKD is not currently available, the congenital polycystic kidney (*cpk*) model a closely mimics the renal and biliary lesions clinically observed in human ARPKD. The *cpk* mouse results from a spontaneous frame shift mutation in the *Cys1* gene, which encodes the protein cystin[11]. Cystin is a myristoylated protein that associates with lipid microdomains in the ciliary membrane and co-localizes with fibrocystin/polyductin complex (FPC), the protein product of *Pkhd1,* as well as a number of other known cystoproteins[12-14]. Current studies in our laboratory have shown that cystin is released from the ciliary membrane by a myristoyl-electrostatic switch mechanism thereby allowing cystin to traffic from the cilium and undergo nuclear import through interactions with importins (Yang, *et al.* 2015 *in preparation*, Watts, *et al.* 2015 *in preparation*)[14].

Recently, we identified the ciliary GTPase Arl3 as a putative interactor of cystin using tandem affinity purification (TAP) (Watts, et al, 2015 *in preparation*). Wright, *et al.* have demonstrated that Arl3 regulates the ciliary entry of cystin and other myristoylated proteins[15]. Interestingly, Arl3 has also been linked to renal cystic disease, as *Arl3*$^{-/-}$ mice are phenotypically similar to the *cpk* mouse, with runting, enlarged, cystic kidneys, and early demise[16]. The phenotypic similarities between the *Arl3*$^{-/-}$ and *cpk* mice, coupled with the identification of Arl3 has a putative interactor of cystin, suggests that cystin and Arl3 may be associated together in a functional pathway.

In the current study, we use CRISPR technology to evaluate the functional interactions between cystin and Arl3, as well as to examine the role of Arl3 in the development of renal cystic disease.

Materials and Methods

CRISPR Constructs

The CRISPR vector, pSpCas9(BB)-2A-GFP (PX458), was a gift from Feng Zhang (Addgene plasmid # 48138)[17]. We used the web-based CRISPR Design tool developed by Massachusetts Institute of Technology (http://crispr.mit.edu/) to generate RNA guides to the early coding region of mouse *Arl3*. The sequence of the guides used in this study are guide a: 5'AAAGGACGAAACACCG-GGAGGTGCGAATCCTACTCC-GTTTAGAGCTAGAA-3' and guide b: 5'-AAAGGACGAAACACCG-GAGGTGCGAATCCTACTCCT-GTTTAGAGCTAGAA-3'. The selected guides were cloned into the CRISPR vector using InFusion cloning (Clontech, 638909) following the manufacturer's protocol.

Nucleofection and Cell Culture

To generate the Arl3^{CRISPR} cell line, one million mIMCD-3 cells (ATCC, CRL-2123) were suspended in 82µL of Nucleofector solution R + 18 µL of supplement (Lonza, VCA-1001) per nucleofection. Then, 5µg of DNA is added to the cell suspension and the program U-017 on the Nucleofector II (Amaxa) was used. The cells were transferred into a six-well dish. As a negative control, the empty CRISPR vector without the RNA guide was used. 18 hours after nucleofection, the cells were sorted by GFP expression to

select for those cells expressing the Cas9::GFP from the CRISPT vector. As a negative control for flow cytometry, mIMCD-3 cells were nucleofected without any CRISPR/guide DNA. The collected GFP-expressing cells, known as Arl3^{CRISPR}, were transferred into a 10cm plate and allowed to grow for five days post-confluence.

The generation of the mTERT immortalized wild type collecting duct cells has been previously described[18]. Using the published method, the *cpk* cell lines were mTERT immortalized in the laboratory of Dr. P. Darwin Bell at the Medical University of South Carolina. The wild type and *cpk* mTERT cells were grown in DMEM/F-12 (Life Technologies, 11320-033) supplemented with 2% heat-inactived FBS, 1% penicillin/streptomycin, 5mL of 100x insulin-transferrin-selenium-G supplement (Sigma-Aldrich, i3146), 0.2 mg/mL Dexamethasone (Sigma-Aldrich, D8893-1MG), and 20nM 3,3',5-Triiodo-L-thyronine sodium salt (Sigma-Aldrich, T6397-100MG) at 39°C.

Lysates were generated using 600µL lysis buffer [30 mM Tris-Cl, pH 7.4, 150 mM NaCl, 0.5% Nonidet P-40 (Fluka, 74385) and protease inhibitor (Roche, 11836170001)]. The cells were collected and incubated with end-over-end rotation for 30 minutes at 4°C and then spun at >15000rpm in a table top centrifuge at 4°C the cleared lysate was used for immunoblotting. The concentration of the lysates generated from the *cpk* mTERT cells were much lower when compared to the wild type mTERT cells, thus the *cpk* lysates were concentrated using Amicon Ultra-4 Centrifugal Filter Unit (EMD Millipore Cat. No. #UFC800324, following manufacture's protocol) to allow for more accurate comparison.

Antibodies and Immunoblotting

For immunoblot analysis, 15µg of lystates were mixed with NuPage sample buffer and reducing agent (LifeTechnologies, NP0007 & NP0009) per manufacturer's protocol to a final volume of 30 µL and were loaded into a Novex 4-12% Bis-Tris pre-cast gel (LifeTechnologies). Following 35 minutes of electrophoresis at 200V, the gels were transferred using the Transblto Tubro Transfer system (BioRad). Membranes were blocked with 5% non-fat milk in PBS + 0.1% Tween20 for one hour at room temperature and then incubated for 12-18 hours with primary antibody diluted to 1:1000 in 5% non-fat milk in PBS + 0.1% Tween20 at 4°C [Arl3:Rabbit anti-Arl3 polyclonal antibody (Protein Tech, 10961-1-AP); c-Myc: Rabbit monoclonal anti-c-Myc antibody (Abcam, ab32072)]. Secondary antibodies were added in 5% non-fat milk in PBS + 0.1% Tween20 for one hour at room temperature.

Cell Cycle Synchronization

To arrest the cell cycle at G_0 the normal growth media of the Arl3^{CRISPR} cells was replaced with serum starvation media (DMEM F/12, 0.5% FBS, 1% Penicillin/Streptomycin) for 48 hours. To arrest the cell cycle at G_1, 40 µM Simvastatin was added to the normal growth media for 24 hours. Each synchronization experiment was performed a total of 3 times.

Results

Comparative pathology

The *Arl3*$^{-/-}$ mice and *cpk* mice share a characteristic ARPKD-like phenotype. They present with abnormal renal, hepatic, pancreatic epithelial ductal structures, increased cell proliferation, and cyst formation (Figure 3.1). The cystic dilatation of the collecting ducts are evident within the first few days of birth, with both *Arl3*$^{-/-}$ and *cpk* mice present with distended abdomens due to bilaterally enlarged kidneys. Both mutant animals show a failure to thrive, dying by 3 weeks of age. In addition to this ARPKD-like renal phenotype, the *Arl3*$^{-/-}$ mice also express glomerular cysts and photoreceptor degeneration by post-natal day 14, which are not evident in the *cpk* mouse (Figure 3.1B, black arrows). These phenotypic similarities, as well as our TAP dataset identifying Arl3 has a putative interactor of cystin, suggests there may be a functional association between cystin and Arl3.

Generation of an in vitro model system using CRISPR-mediated knockdown of Arl3

To define the putative relationship between cystin and Arl3, we utilized CRISPR technology to knockdown Arl3 expression in mIMCD-3 cells, thereby generating an *in vitro* model that would mimic the *Arl3*$^{-/-}$ mouse, allowing us to further assess the physiological changes that result in the absence of Arl3.

Using CRISPR technology, we generated a cell line wherein Arl3 was disrupted using unique RNA guides specific to mouse *Arl3* exon 1. An Arl3^{CRISPR} cell line was then generated by introducing the CRISPR vectors that expressed both the unique guide sequences and Cas9::GFP into mIMCD-3 cells via nucleofection. The expression levels of

Arl3 were evaluated in the Arl3^{CRISPR} cells by immunoblotting to assess the efficacy of our *in vitro* approach. As shown in Figure 3.2B, *Arl3* expression was successfully reduced by ~98% in the Arl3^{CRISPR} cells when compared to the negative control, indicating that the cells had indeed undergone genomic editing by the *Arl3*-targeting CRISPR vector. These data confirm that we have generated a viable *in vitro* cell system with near complete ablation of *Arl3* expression.

CRISPR-mediated knockdown of Arl3 results in increased c-Myc expression

Increased c-Myc expression was first observed in the kidneys of the *cpk* mouse, and has subsequently become a hallmark characteristic of cystic epithelia[19-30]. However, the kidney is a complex organ composed of a number of diverse cell types, as well as vasculature and mesenchymal elements. In both human ARPKD and the *cpk* mouse model, renal cystogenesis predominantly involves cystic dilatation of the collecting duct. Therefore, we assessed the expression levels of c-Myc in immortalized collecting duct cell lines from wild type and *cpk* mice (henceforth referred to as wild type and *cpk* mTERT cells, respectively), an *in vitro* system more specific to ARPKD[18].

The wild type and *cpk* mTERT cells were grown for 5 days post-confluence and lysed. Equal amounts of protein were subjected to SDS-PAGE and immunoblot analysis using antibodies against c-Myc. The analysis shows that the expression of c-Myc is significantly elevated in the *cpk* mTERT cells as compared to the wild type control (Figure 3.3A). These data confirm the initial observation made by Cowley *et al.* in 1991 that c-Myc expression is elevated in *cpk* kidneys and is in accordance with previously published

data from our laboratory that demonstrated c-Myc overexpression in the absence of cystin[31].

We next evaluated c-Myc expression in our Arl3^{CRISPR} cell system. In order to reduce the heterogeneity of the cell population, we used serum starvation to synchronize the cell cycle at G_0 and induce growth of the primary cilium[32, 33]. Immunoblot analysis of the cell lysates indicated a significant increase in c-Myc expression in the Arl3^{CRISPR} cells compared to the negative control (Figure 3.3B). To confirm these data, we also used simvastatin, a member of the 3-hydroxy-3-methylglutarylcoenzyme CoA (HMG-CoA) reductase inhibitor class of drugs, which also includes lovastatin. Previous studies have demonstrated that both simvastatin and lovastatin can be used interchangeably to arrest the cell cycle at the G_1 phase[34]. The Arl3^{CRISPR} cells were treated with 40μM simvastatin for 24 hours[35]. As with the serum starvation experiments, immunoblot analysis reveals significantly increased c-Myc levels in the Arl3^{CRSIPR} cells as compared with the negative control (Figure 3.3C). Having demonstrated that the loss of Arl3 results in increased c-Myc expression in our Arl3^{CRISPR} cell system, we next examined the influence of cystin on the elevated levels of c-Myc.

Cystin can attenuate c-Myc expression levels in Arl3^{CRISPR} cells

Previous published data from our lab demonstrates that cystin can regulate c-Myc expression through its nuclear interaction with necdin[31]. Having demonstrated that the loss of Arl3 results in increased c-Myc expression in our Arl3^{CRISPR} cell system, we next examined the influence of cystin on the elevated levels of c-Myc. To this end, we exogenously overexpressed a TAP-tagged, myristoylation deficient cystin mutant, NSFTAP-

cystin, which was previously described, in our Arl3^{CRISPR} cells grown under serum starvation (Watts, *et al.* 2015 *in preparation*). As shown in Figure 3.4, preliminary immunoblot analysis of the cell lysates indicates that the overexpression of NSFTAP-cystin attenuates the expression of c-Myc in our Arl3^{CRISPR} cells reducing the expression to endogenous levels as indicated by the negative control (black bar). Additionally, overexpression of cystin can also reduce the expression of c-Myc to below endogenous levels in our Arl3^{CRISPR} cells, confirming the work done by Wu *et al.*. Together, these data demonstrate that Arl3 and cystin have a functional interaction and, together, regulate c-Myc expression.

Discussion

In recent studies, we used a TAP protocol to identify cystin interacting partners in order to further elucidate the cellular functions of this recessive PKD-associated protein. While our dataset was enriched for proteins involved in nuclear import and function, proteins from several other subcellular compartments were also identified. Among these putative interacting partners, the ciliary GTPase, Arl3, emerged as a promising candidate for further study.

Several studies have identified Arl3 as a key factor in the maintenance and regulation of membrane-associated ciliary proteins[16, 36-38]. Work by Wright *et al.* have implicated Arl3 as a regulator of ciliary localization of myristoylated-proteins. The protein of interest in their study was Nphp3, a myristoylated cystoprotein linked to the hepatorenal fibrocystic disease, nephronophthisis. Cystin, another myristoylated cystroprotein, was used for proof of concept, further supporting their proposed model for the involve-

ment of Arl3 in ciliary localization of myristoylated proteins[15]. In Figure 3.5A, we present a modified version of the model proposed by Wright *et al.* based on the data generated in the current study.

In wild type cells, cystin is transcribed on soluble ribosomes where it undergoes enzymatically driven, cotranslational, N-terminal myristoylation[14, 39]. Once cystin has been transcribed, UNC119b, a protein that possesses a hydrophobic pocket that accommodates lipid moieties of membrane-associated, post-translationally modified proteins, binds to cystin via its myristoyl moiety[15, 40-42]. UNC119b is characterized as a member of the 'GDI-like solubilizing factor' family, a group of proteins that have been implicated in ciliary trafficking of lipid-modified proteins[41, 43, 44]. The UNC119b/cystin complex is trafficked to and internalized by the cilium through a yet to be defined mechanism. Once inside the cilium, Arl3 binds to the UNC119b/cystin complex, causing a conformational change in the hydrophobic pocket of UNC119b, stimulating the release of cystin, and thereby allowing for the association of cystin with lipid microdomains within the ciliary membrane. Following the release of cystin, RP2, the GTPase activating protein (GAP) of Arl3, activates Arl3 GTPase activity, which causes the dissociation of Arl3 and UNC119b, with the latter protein subsequently trafficked out of the cilium.

The function of cystin within the cilium remains unclear; however, work from our group has established that cystin contains both an active myristoylation domain and polybasic domain. We propose that cystin undergoes regulated release from the ciliary membrane via a myristoyl-electrostatic switch after phosphorylation, as has been described for the MARCKS proteins[45]. Once free of the ciliary membrane, cystin exits the cilium

and traffics to the nucleus, where it functions to regulate c-Myc expression, and may have a role in regulating splicing (Watts, et al. 2015 *in preparation*)[31].

We predict that in our Arl3^{CRISPR} *in vitro* system, the initial processes of the regulated localization of cystin would remain intact. Cystin would undergo cotranslational N-terminal myristoylation and be bound by UNC119b, and the UNC119b/cystin complex would then be targeted to the cilium. However, as depicted in Figure 3.5B, in the absence of Arl3, cystin would remain bound to UNC119b. The inability of cystin to be released from UNC119b would lead to its functional sequestration, thereby disrupting the physiological functions of cystin. This functional sequestration appears to phenocopy the loss of cystin, leading to a dysregulation of c-Myc expression, as is observed in the *cpk* mTERT cells and the *cpk* mouse kidney. Based on the data presented in the current study, we predict that the cystic phenotype observed in the *Arl3*$^{-/-}$ mouse results, at least in part, from a dysregulation of c-Myc expression due to the loss of functional cystin. We propose that the phenotypic distinctions in the *Arl3*$^{-/-}$ mouse, such as glomerular cysts and photoreceptor degeneration, may result from a dysregulation in the ciliary localization of other ciliary proteins, such as Nphp3.

Taken together, our data support the hypothesis that Arl3 serves a critical role in the localization and physiological regulation of cystin. We have demonstrated that at a cellular level disruptions in Arl3 expression mimic the loss of cystin and may contribute to epithelial cystogenesis, at least in part, through a dysregulation of c-Myc expression. These findings suggest that cystin and Arl3 are involved in a molecular complex required to maintain normal ciliary signaling and renal epithelial differentiation. Further *in vivo*

studies are required to elucidate the mechanisms through which cystin dysregulation contributes to Arl3-related renal cystogenesis.

Acknowledgments

We thank Troy McEachron, PhD, formerly of the Pan laboratory at Children's National Health System for generously providing CRISPR and nucleofection technical advice. Special thanks to Naoe Harafuji, PhD for experimental support, as well as Lina Chakrabarti, PhD and Christopher Lazarski, PhD for their assistance with flow cytometry. Our thanks to the Zeichner laboratory at Children's National Health System for providing the simvastatin used in this study. Finally, the authors are grateful to Amber K. O'Connor, PhD of akoWriting, LLC for critically reviewing this manuscript.

References:

1. Pazour, G.J., *Intraflagellar transport and cilia-dependent renal disease: the ciliary hypothesis of polycystic kidney disease.* J Am Soc Nephrol, 2004. **15**(10): p. 2528-36.
2. Badano, J.L., et al., *The ciliopathies: an emerging class of human genetic disorders.* Annu Rev Genomics Hum Genet, 2006. **7**: p. 125-48.
3. Hildebrandt, F., M. Attanasio, and E. Otto, *Nephronophthisis: disease mechanisms of a ciliopathy.* J Am Soc Nephrol, 2009. **20**(1): p. 23-35.
4. Kerkar, N., K. Norton, and F.J. Suchy, *The hepatic fibrocystic diseases.* Clin Liver Dis, 2006. **10**(1): p. 55-71, v-vi.
5. Gunay-Aygun, M., *Liver and kidney disease in ciliopathies.* Am J Med Genet C Semin Med Genet, 2009. **151C**(4): p. 296-306.
6. Guay-Woodford, L.M., *Autosomal recessive polycystic kidney disease: the prototype of the hepato-renal fibrocystic diseases.* J Pediatr Genet, 2014. **3**(2): p. 89-101.
7. Ward, C.J., et al., *The gene mutated in autosomal recessive polycystic kidney disease encodes a large, receptor-like protein.* Nat Genet, 2002. **30**(3): p. 259-69.
8. Onuchic, L.F., et al., *PKHD1, the polycystic kidney and hepatic disease 1 gene, encodes a novel large protein containing multiple immunoglobulin-like plexin-transcription-factor domains and parallel beta-helix 1 repeats.* Am J Hum Genet, 2002. **70**(5): p. 1305-17.

9. Zerres, K., et al., *Prenatal diagnosis of autosomal recessive polycystic kidney disease (ARPKD): molecular genetics, clinical experience, and fetal morphology.* Am J Med Genet, 1998. **76**(2): p. 137-44.
10. Harris, P. and V. Torres, *Polycystic kidney disease.* Annu Rev Med, 2009. **60**: p. 321-37.
11. Hou, X., et al., *Cystin, a novel cilia-associated protein, is disrupted in the cpk mouse model of polycystic kidney disease.* J Clin Invest, 2002. **109**(4): p. 533-40.
12. Somlo, S., Guay-Woodford L., *Genetic Diseases of the Kidney*. First ed2009: Elsevier.
13. Yoder, B., X. Hou, and L. Guay-Woodford, *The polycystic kidney disease proteins, polycystin-1, polycystin-2, polaris, and cystin, are co-localized in renal cilia.* J Am Soc Nephrol, 2002. **13**(10): p. 2508-16.
14. Tao, B., et al., *Cystin localizes to primary cilia via membrane microdomains and a targeting motif.* J Am Soc Nephrol, 2009. **20**(12): p. 2570-80.
15. Wright, K.J., et al., *An ARL3-UNC119-RP2 GTPase cycle targets myristoylated NPHP3 to the primary cilium.* Genes Dev, 2011. **25**(22): p. 2347-60.
16. Schrick, J.J., et al., *ADP-ribosylation factor-like 3 is involved in kidney and photoreceptor development.* Am J Pathol, 2006. **168**(4): p. 1288-98.
17. Ran, F.A., et al., *Genome engineering using the CRISPR-Cas9 system.* Nat Protoc, 2013. **8**(11): p. 2281-308.
18. Steele, S.L., et al., *Telomerase immortalization of principal cells from mouse collecting duct.* Am J Physiol Renal Physiol, 2010. **299**(6): p. F1507-14.
19. Cowley, B.J., et al., *Elevated proto-oncogene expression in polycystic kidneys of the C57BL/6J (cpk) mouse.* J Am Soc Nephrol, 1991. **1**(8): p. 1048-53.
20. Burn, T.C., et al., *Increased exon-trapping efficiency through modifications to the pSPL3 splicing vector.* Gene, 1995. **161**(2): p. 183-7.
21. Ramirez-Solis, R., P. Liu, and A. Bradley, *Chromosome engineering in mice.* Nature, 1995. **378**(6558): p. 720-4.
22. Smith, A.J., et al., *A site-directed chromosomal translocation induced in embryonic stem cells by Cre-loxP recombination.* Nat Genet, 1995. **9**(4): p. 376-85.
23. Perez, I., et al., *Mutation of PTB binding sites causes misregulation of alternative 3' splice site selection in vivo.* RNA, 1997. **3**(7): p. 764-78.
24. Cleary, M.A., et al., *Disruption of an imprinted gene cluster by a targeted chromosomal translocation in mice.* Nat Genet, 2001. **29**(1): p. 78-82.
25. Valenzuela, D.M., et al., *High-throughput engineering of the mouse genome coupled with high-resolution expression analysis.* Nat Biotechnol, 2003. **21**(6): p. 652-9.
26. Yeo, G., et al., *Variation in sequence and organization of splicing regulatory elements in vertebrate genes.* Proc Natl Acad Sci U S A, 2004. **101**(44): p. 15700-5.
27. Yeo, G.W., et al., *Identification and analysis of alternative splicing events conserved in human and mouse.* Proc Natl Acad Sci U S A, 2005. **102**(8): p. 2850-5.

28. Williams, S.S., et al., *Kidney cysts, pancreatic cysts, and biliary disease in a mouse model of autosomal recessive polycystic kidney disease.* Pediatr Nephrol, 2008. **23**(5): p. 733-41.
29. Bakeberg, J.L., et al., *Epitope-tagged Pkhd1 tracks the processing, secretion, and localization of fibrocystin.* J Am Soc Nephrol, 2011. **22**(12): p. 2266-77.
30. Skarnes, W.C., et al., *A conditional knockout resource for the genome-wide study of mouse gene function.* Nature, 2011. **474**(7351): p. 337-42.
31. Wu, M., et al., *The ciliary protein cystin forms a regulatory complex with necdin to modulate Myc expression.* PLoS One, 2013. **8**(12): p. e83062.
32. Chen, M., et al., *Serum starvation induced cell cycle synchronization facilitates human somatic cells reprogramming.* PLoS One, 2012. **7**(4): p. e28203.
33. Harada, A., et al., *Golgi vesiculation and lysosome dispersion in cells lacking cytoplasmic dynein.* J Cell Biol, 1998. **141**(1): p. 51-9.
34. Liang, Y.W., et al., *Preclinical Activity of Simvastatin Induces Cell Cycle Arrest in G1 via Blockade of Cyclin D-Cdk4 Expression in Non-Small Cell Lung Cancer (NSCLC).* Int J Mol Sci, 2013. **14**(3): p. 5806-16.
35. Javanmoghadam-Kamrani, S. and K. Keyomarsi, *Synchronization of the cell cycle using lovastatin.* Cell Cycle, 2008. **7**(15): p. 2434-40.
36. Schwarz, N., A.J. Hardcastle, and M.E. Cheetham, *Arl3 and RP2 mediated assembly and traffic of membrane associated cilia proteins.* Vision Res, 2012. **75**: p. 2-4.
37. Veltel, S., et al., *The retinitis pigmentosa 2 gene product is a GTPase-activating protein for Arf-like 3.* Nat Struct Mol Biol, 2008. **15**(4): p. 373-80.
38. Kim, H., et al., *Ciliary membrane proteins traffic through the Golgi via a Rabep1/GGA1/Arl3-dependent mechanism.* Nat Commun, 2014. **5**: p. 5482.
39. Bijlmakers, M.J., *Protein acylation and localization in T cell signaling (Review).* Mol Membr Biol, 2009. **26**(1): p. 93-103.
40. Hanzal-Bayer, M., et al., *The complex of Arl2-GTP and PDE delta: from structure to function.* EMBO J, 2002. **21**(9): p. 2095-106.
41. Ismail, S.A., et al., *Arl2-GTP and Arl3-GTP regulate a GDI-like transport system for farnesylated cargo.* Nat Chem Biol, 2011. **7**(12): p. 942-9.
42. Zhang, H., et al., *UNC119 is required for G protein trafficking in sensory neurons.* Nat Neurosci, 2011. **14**(7): p. 874-80.
43. Chandra, A., et al., *The GDI-like solubilizing factor PDEdelta sustains the spatial organization and signalling of Ras family proteins.* Nat Cell Biol, 2012. **14**(2): p. 148-58.
44. Ismail, S.A., et al., *Structural basis for Arl3-specific release of myristoylated ciliary cargo from UNC119.* EMBO J, 2012. **31**(20): p. 4085-94.
45. McLaughlin, S. and A. Aderem, *The myristoyl-electrostatic switch: a modulator of reversible protein-membrane interactions.* Trends Biochem Sci, 1995. **20**(7): p. 272-6.
46. Wilson, P.D., *Polycystic kidney disease.* N Engl J Med, 2004. **350**(2): p. 151-64.

Figure 3.1: Comparative histopathology. While both the *Arl3*$^{-/-}$ and *cpk* mouse models express collecting duct cysts (red arrows) similar to ARPKD, the *Arl3*$^{-/-}$ mouse also has glomerular cysts (black arrows) and photoreceptor degeneration, both features which are are not observed in either human ARPKD or the *cpk* mouse.

Panel A: Reproduced with permission from [46], Copyright Massachusetts Medical Society

Panel B: Reprinted from "ADP-ribosylation factor-like 3 is involved in kidney and photoreceptor development." *The American Journal of Pathology* 2006 Apr;168(4):1288-98. Used with permission by Elsevier

Figure 3.2: CRISPR-mediated knockdown of *Arl3*. (A) Schematic representation of the CRISPR guide alignment to the coding sequence of mouse *Arl3*. (B) Immunoblot analysis of *Arl3* knockdown in our *Arl3*^{CRISPR} cells. Guides A, B, and a no-guide negative control where nucleofected into mIMCD-3 cells, sorted, and the cells were then allowed to grow for 5 days post-confluence. After lysis, equal protein amounts from each lysate were evaluated. The expression of Arl3 was effectively reduced by nearly 98% in the *Arl3*^{CRISPR} cells when compared to the negative control. GAPDH was used as a loading control. The figure represents n=3 experiments.

Figure 3.3: c-Myc expression in cell lines. (A and B) Immunoblot analysis demonstrates increased c-Myc expression in *cpk* versus wild type mTERT cell lines. (C and D) c-Myc levels are significantly increased in Arl3^{CRISPR} cells after cell cycle synchronization and primary cilium growth induction following 24 hour serum starvation. (E and F) As con-

firmation, Arl3^{CRISPR} cells treated with simvastatin, which causes cell cycle arrest and results in cell cycle synchronization, again demonstrated an increase in c-Myc expression.

Figure 3.4: Cystin attenuation of elevated c-Myc expression. Immunoblot analysis using antibodies against c-Myc show that c-Myc levels are elevated in the Arl3^{CRISPR} cells and can be reduced to endogenous levels (black bar) through the exogenous overexpression of NSFTAP-cystin. This figure represents preliminary studies, n=2.

Figure 3.5: Schematic model of Arl3 regulation of cystin localization. (A) In wild type cells, UNC119b binds to the myristoylation domain of cystin and shuttles it to the cilium. Arl3 binds to UNC119b, stimulating the release of cystin from UNC119b. Cystin is then able to associate with lipid-raft microdomains within the membrane via its myristoyl-group and anchor to the ciliary membrane. Through regulatory mechanisms that have yet to be defined, cystin can be phosphorylated at S17, stimulating its release from the ciliary membrane and facilitating its trafficking into the nucleus where it can regulate c-Myc expression. (B) In our Arl3^{CRISPR} cell system, cystin would be trafficked to the cilium by UNC119b. However, without Arl3 present to stimulate the release of cystin from UNC119b, the UNC119b/cystin complex remains intact. The inability of cystin to be released from UNC119b causes a functional sequestration that disrupts cystin association with the ciliary membrane and its regulated trafficking to the nucleus. This functional sequestration would mimic a loss of cystin protein, thus recapitulating the cellular signature of cystic epithelial, namely the overexpression of c-Myc.

Figure 3.1

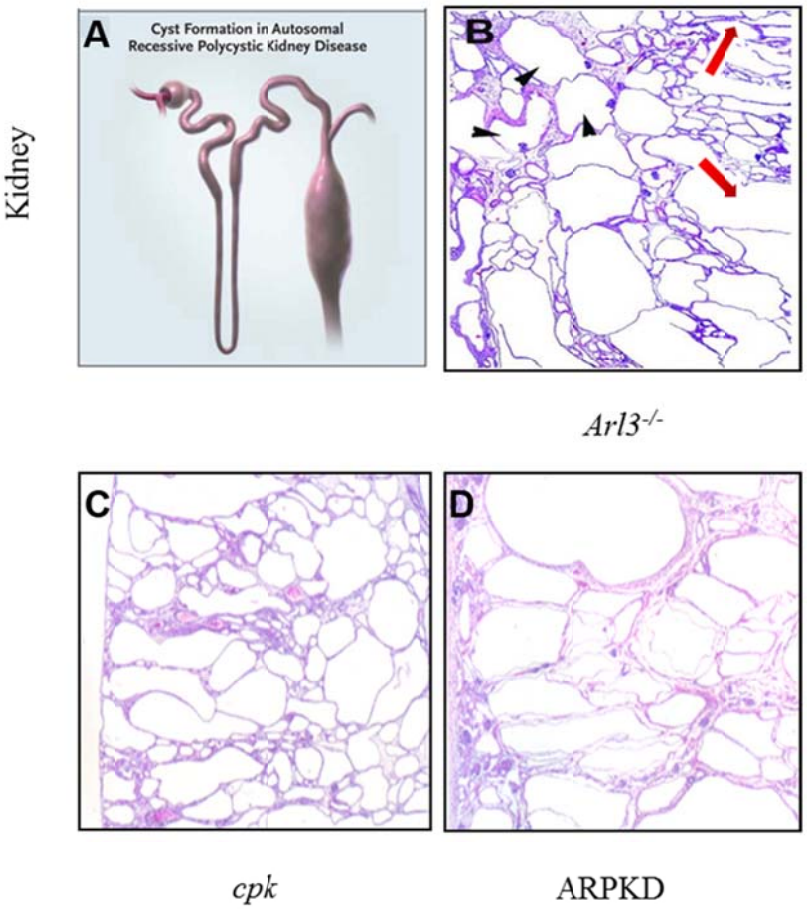
Kidney
A
Cyst Formation in Autosomal Recessive Polycystic Kidney Disease
B
Arl3-/-
C
D
cpk
ARPKD

Figure 3.2

A


40
70
3' …CCAGACCAGGAGGTGCGAATCCTACTCCTGG… 5'
Guide A - GGAGGTGCGAATCCTACTCC
Guide B - GAGGTGCGAATCCTACTCCT

B

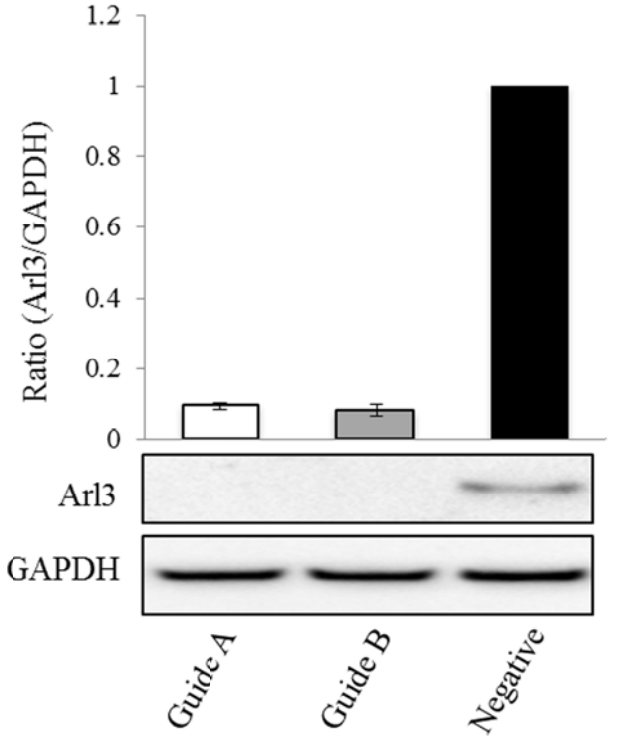
Ratio (Arl3/GAPDH)
1.2
1
0.8
0.6
0.4
0.2
0
Arl3
GAPDH
Guide A
Guide B
Negative

Figure 3.3

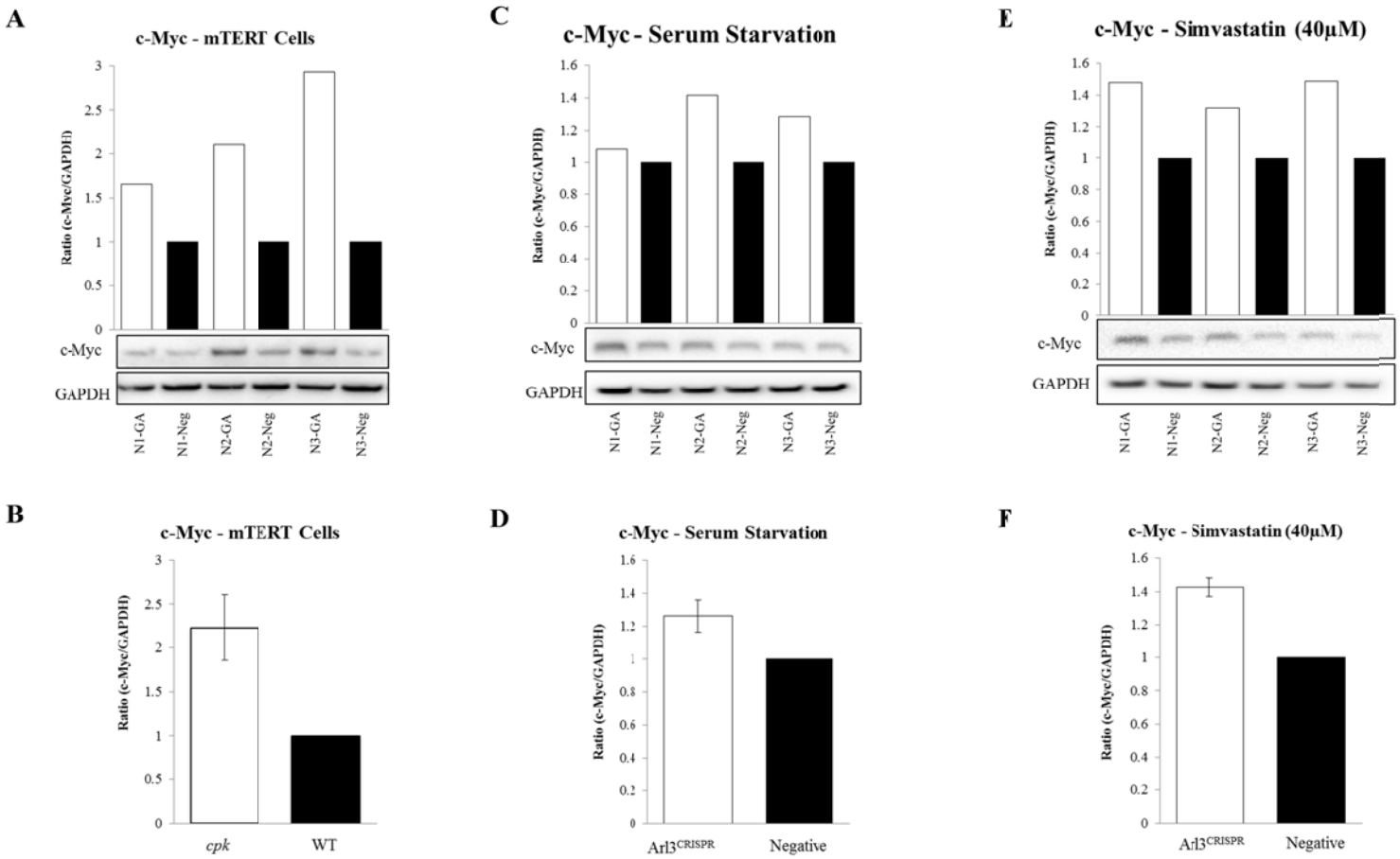
A
c-Myc - mTERT Cells
Ratio (c-Myc/GAPDH)
c-Myc
GAPDH
N1-GA
N1-Neg
N2-GA
N2-Neg
N3-GA
N3-Neg
B
c-Myc - mTERT Cells
Ratio (c-Myc/GAPDH)
cpk
WT
C
c-Myc - Serum Starvation
D
c-Myc - Serum Starvation
Arl3CRISPR
Negative
E
c-Myc - Simvastatin (40µM)
F
c-Myc - Simvastatin (40µM)

Figure 3.4

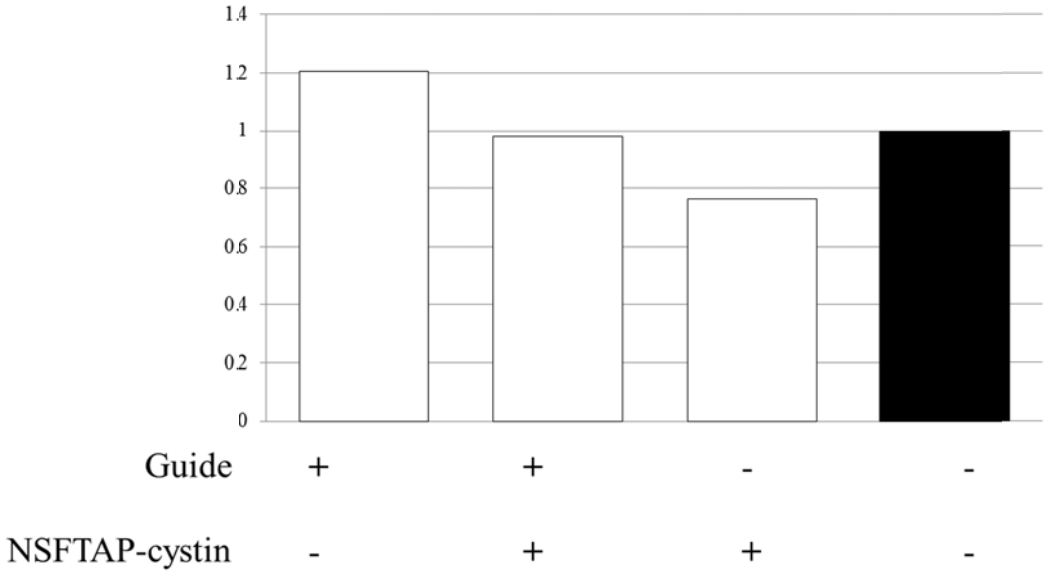

Figure 3.4

A.) Wild Type

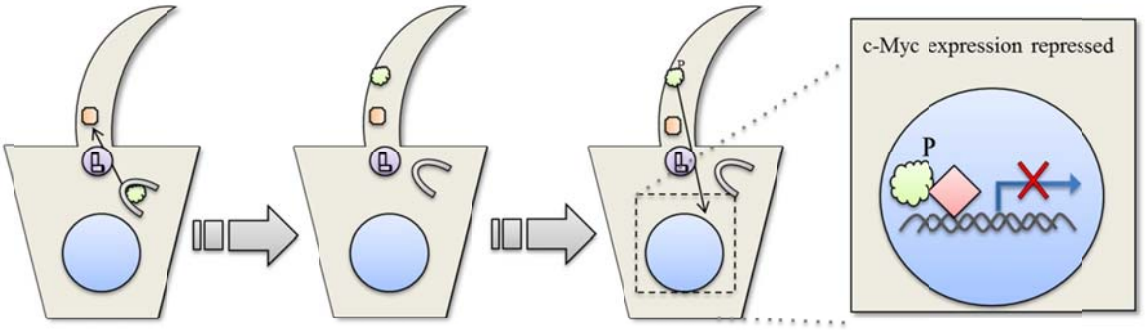

B.) CRISPR knockdown of Arl3

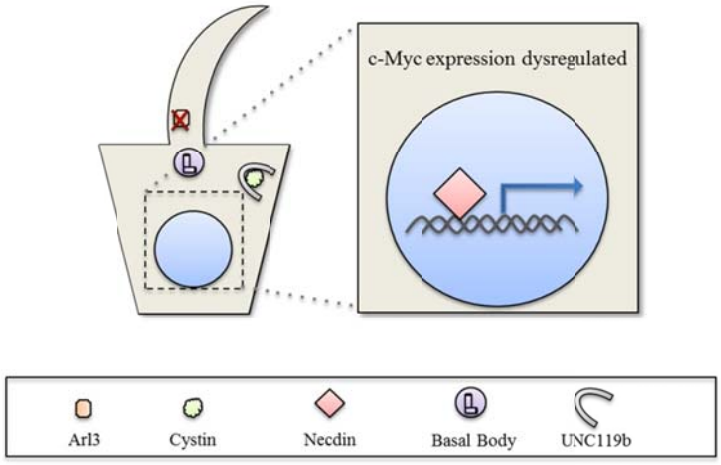

CHAPTER 4

CONCLUSIONS AND FUTURE DIRECTIONS

The Trafficking of Cystin to and from the Cilium

Our data indicates that cystin localizes to the primary cilium through the coordinated function of the myristoylation domain and the unique ciliary localization signal[71]. Although the ciliary localization of cystin has been confirmed through a number of studies, the specific mechanism by which cystin enters the cilium remains unknown. Interestingly, the studies described in this dissertation demonstrate a direct interaction between cystin and Importin β2 through GST-pulldown experiments (Figure 2.4). Previous studies have linked the ciliary import of the kinesin motor protein Kif17, as well as the retinitis pigmentosa 2 (RPS) protein to Importin β2[84, 85]. These data suggest that, like Kif17 and RP2, the ciliary entry of cystin may also be regulated by its interaction with Importin β2. Further investigation will be required to determine the specific molecular domains involved in the cystin and Importin β2 interaction.

While we have begun to identify some of the entry pathways for cystin ciliary localization, the molecular mechanisms by which cystin exits the cilium are still unknown. One hypothesis involves endocytosis at the ciliary pocket, a membrane domain found at the base of both primary and motile cilia (Figure 1.1). The ciliary pocket was first observed over 50 years ago, but was subsequently ignored. However, recent experimental studies have reinvigorated interest in its functional role in ciliary trafficking[86]. The ciliary pocket was named after its morphological and functional similarities with the fla-

gellar pocket, a unique site for endocytosis and exocytosis in Trypanosomes, a flagellated protozoan [87]. In Trypanosomes, membrane proteins are internalized by clathrin-mediated endocytosis from the ciliary pocket[87, 88]. Likewise, in mice, the ciliary pocket has been linked to vesicular trafficking, and is often characterized by a high density of budding clathrin-coated pits, suggesting that the ciliary pocket is involved in clathrin-mediated endocytosis[89-91]. Indeed, endocytosis at the level of the ciliary pocket has been proposed as a mechanism by which proteins exit the cilium and are subsequently internalized into the cell, either for degradation, intracellular function, or recycling.

A number of proteins involved in endocytosis were identified in our cystin TAP dataset, further supporting the thesis that endocytosis may be involved in the internalization of cystin from the ciliary membrane. We identified several components of the adaptor protein complex 2 (AP2), a protein complex involved in the clathrin-mediated endocytosis through cargo selection and vesicle formation[92, 93]. We also identified many members of the Rab family of proteins, including Rab5c and Rab11, which are responsible for regulating early endosome formation and recycling endosomes, respectively[94]. The presence of these and other endocytic proteins begs the question: does cystin exit the cilium through clathrin-mediated endocytosis following membrane dissociation via the myristoyl-electrostatic switch? Further characterization of the molecular complexes involving cystin and these endocytic proteins is required. If successful, these studies could provide critical insights into the mechanistic pathways for ciliary exit , which is critical in furthering our understanding of the trafficking dynamics of cystin, as well as other ciliary proteins.

Intracellular Trafficking and Nuclear Localization of Cystin

Our TAP-based studies identified the ciliary GTPase, Arl3, as a putative interacting partner of cystin. This observation is notable for several reasons. First, *Arl3*$^{-/-}$ mice present with renal and biliary phenotypes that are very similar to the phenotypes described in the *cpk* mouse[95]. Second, Arl3 has been identified as a critical protein for ciliary localization[96]. Third, in the study by Wright *et al*., Arl3 was shown to stimulate the release of cystin from UNC119b within the cilium[96]. Taken together, these data suggest that cystin and Arl3 may function together in a molecular complex that is critical for the ciliary localization and function of cystin.

In an effort to define this molecular complex, we utilized CRISPR technology to create an *in vitro* system with reduced Arl3 expression. Immunoblot analyses of the resulting cells, Arl3^{CRISPR}, showed ~98% reduction in Arl3 expression, as well as elevated levels of c-Myc expression. Corroborating these data, the expression levels of c-Myc were also elevated in the *cpk* mTERT cells, an immortalized collecting duct cell line harvested from the collecting ducts of *cpk* mice. These data are concordant with previously published studies that demonstrated elevated c-Myc expression as a hallmark feature of cystic epithelia[74].

These findings, together with the data demonstrating that cystin regulates c-Myc expression, help to define a putative model which expands on the work described by Wright *et al.*[72, 96]. In a wild type system, cystin is translated and undergoes N-terminal myristoylation. UNC119b, via a hydrophobic pocket in the protein's structure, binds to the myristoylation domain of cystin. This UNC119b/cystin complex is then trafficked into the cilium through an as yet to be defined mechanism. Within the cilium,

Arl3 binds to UNC119b causing a conformational change in the hydrophobic pocket that results in the release of cystin. Arl3 via its GTPase activity, which is activated by RP2, then dissociates from UNC119b, which is subsequently trafficked out of the cilium. Although its precise ciliary function remains unknown, the released cystin associates with lipid microdomains within the ciliary membrane (Figure 3.4A).

In our Arl3^{CRISPR} *in vitro* model, we propose that the UNB119b/cystin complex remains intact due to the loss of Arl3. Thus, cystin is functionally sequestered and, therefore, is unable to associate with the ciliary membrane or undergo regulation via its myristoyl-electrostatic switch. We speculate that this functional sequestration of cystin phenocopies the loss of cystin, leading to elevated c-Myc expression, which likely contributes to the renal cystic phenotype observed in the *cpk* and *Arl3*$^{-/-}$ mouse (Figure 3.4B).

In order for cystin to traffic to the nucleus, it must be undergo regulated release from the cilium, likely via the myristoyl-electrostatic switch mechanism, a well-studied molecular mechanism used to release membrane associated proteins[73]. The myristoylation and polybasic domains within cystin work in concert with one another to anchor cystin into the ciliary membrane. In addition, recent data from our laboratory demonstrates that the kinase EPAC phosphorylates cystin at serine 17, which is positioned immediately adjacent to the polybasic domain, RRRRS (amino acids 13-17). This phosphorylation event causes a change in the overall charge of the region, weakening the membrane association, resulting in the release of cystin from the ciliary membrane. Once released, cystin exits the cilium through an as yet undefined mechanism, and is imported into the nucleus where it is involved in transcriptional regulation, *e.g.*, c-Myc expression.

Our TAP studies have identified multiple importin subunits as putative interactors of cystin, and through GST-pulldown experiments, we were able to confirm direct interactions between cystin and several of the importin subunits. These data suggest that cystin undergoes active nuclear import rather than passive diffusion, suggesting that its nuclear import is a regulated process.

Cystin and Transcriptional Regulation

The data presented in Chapter 3 of this dissertation both confirms and expands on data previously published from our laboratory demonstrating that cystin is able to regulate gene expression through interactions with other proteins[72]. However, Wu *et al.* also made another intriguing observation. In addition to binding with necdin, cystin was able to bind to DNA independently, despite the absence of known DNA binding domains[72]. This ability to bind DNA suggests that cystin may be able to regulate the expression of other genes directly, as well as through interactions with other proteins.

To explore this provocative hypothesis, ChIP-Seq could be used to further define the transcriptome regulated by cystin. ChIP-Seq allows for the identification of regions of DNA bound by DNA binding proteins on a genome-wide scale. Using the results from the ChIP-Seq experiments, microarray analyses could then be performed to assess changes in the expression levels of these genes in mTERT immortalized collecting duct cells derived from wild type and *cpk* kidneys. Identifying and understanding the genes whose transcription is dysregulated as a result of a loss of cystin function would provide new insights into the molecular mechanisms that underlie the pathobiology of ARPKD. These experiments would offer critical insights into the onset and progression of the disease,

helping clinical investigators to refine genetic testing methodologies, identify new genetic modifiers, ascertain why certain mutations are more deleterious or pathogenic than others, and perhaps identify potential therapeutic targets that could be developed for directed interventions.

Cystin and Splicing Regulation

Data presented in this dissertation demonstrates a putative difference in the transcriptional profile of *Pkhd1*, the mouse orthologue of the disease gene involved in human ARPKD, in collecting duct cells derived from wild-type and *Cys1*$^{cpk/cpk}$ kidneys. Changes to the *Pkhd1* transcriptional profile in the absence of cystin may contribute to the cystogenesis observed in the *cpk* mouse. The TAP data presented in Chapter 2 suggests that cystin may interact with proteins involved in the regulation of splicing, as approximately 25% of the cystin nuclear interactome identified using TAP is comprised of proteins related to splicing (Figure 2.3, green nodes; Table 2.1). Our initial data suggest that when cystin is absent or rendered non-functional, either through sequestration or mutational disruption, the splicing of *Pkhd1* is dysregulated. The loss of cystin function appears to result in transcriptional changes that mirror certain *Pkhd1/PKHD1* point mutations that affect SRSF binding motifs required for properly regulated splicing to occur. As described by Boddu *et al.*, alternations to these SRSF motifs can cause defects in the splicing of *Pkhd1/PKHD1* that could contribute to renal cystic disease pathogenesis[42].

These data suggest that the cystic phenotype observed in the *cpk* mouse may be the cumulative effect of c-Myc overexpression and perturbations in the splicing of *Pkhd1*, both resulting from an absence of functional cystin. Further studies are required to estab-

lish the molecular connection between cystin and splicing regulation. High-throughput next generation sequencing technologies, such as RNA-Seq, may provide an important tool for such studies. A comparison of transcripts from the mTERT-immortalized collecting duct cells from wild type and *cpk* mice could help define the differential *Pkhd1* expression profile that results in the absence of cystin function. Such studies would provide new insights into the consequences of the loss of cystin on *Pkhd1* alternative splicing. Furthermore, analysis of these alternatively spliced transcripts could help establish mechanisms that distinguish disease-related processes from normal physiological pathways, thus broadening our understanding of the diverse phenotypic heterogeneity observed in ARPKD patients.

Cystin and Fibrocystin/Polyductin Complex

The regulated localization of cystin to the cilium and the nucleus suggests that cystin serves a critical function within both subcellular compartments. FPC has been shown by our laboratory and others to localize to the primary cilium, where it undergoes Notch-like processing, resulting in the release of a C-terminal fragment, which localizes to the nucleus[55]. These molecular data, coupled with the phenotypic similarities between human ARPKD and the *cpk* mouse suggest that cystin and FPC are functionally connected. However the validity of this connection remains to be established at a molecular level. The large molecular weight and transcriptional complexity of FPC have complicated the generation of robust immunoreagents, thereby limiting directed functional studies. The methods described in this dissertation offer a promising approach to begin to assess the functions of FPC within the nucleus. Future studies aimed at performing

TAP using a C-terminal fragment of FPC would allow for the characterization of the nuclear interactome of FPC. As with cystin, this putative nuclear interactome would provide novel insights into the nuclear function of FPC. Specifically, comparison of these two nuclear interactomes may identify transcriptional targets that are common to cystin and FPC and/or establish a hierarchy of transcriptional function between cystin and FPC isoforms, offering the first evidence as to why the non-orthologous *cpk* mouse model so accurately phenocopies ARPKD.

Summary

The principal goal of this work was to broaden our understanding regarding the nuclear import and function of cystin, the protein disrupted in the *cpk* mouse model of recessive polycystic kidney disease. Through GST-pulldown experiments, we have been able to confirm a direct connection between cystin and the importin proteins, as suggested by TAP, providing the first evidence of a mechanism for the nuclear import of cystin. We have also been able to further elucidate the nuclear function of cystin to include a potential role for cystin in splicing regulation, complementing studies our previous studies demonstrating its role in regulating c-Myc gene expression.

Our TAP studies have allowed us to identify and characterize a novel functional interaction between cystin and Arl3, which highlights the importance of cystin's ciliary localization for its physiological regulation and function. Finally, the dataset generated from our TAP studies offers an array of putative interactions with endocytic pathway proteins that will provide further insight into the molecular functions of cystin.

In summary, the data presented in this dissertation substantiates the use of large-scale protein identification techniques as an effective method for elucidating unknown protein functions through protein associations. Indeed, the true power of TAP lies in its capacity to generate an extensive dataset that may serve as the foundational basis for specific hypothesis generation and numerous future functional studies.

LIST OF GENERAL REFERENCES

1. Fliegauf, M., T. Benzing, and H. Omran, *When cilia go bad: cilia defects and ciliopathies.* Nat Rev Mol Cell Biol, 2007. **8**(11): p. 880-93.
2. Emmer, B.T., D. Maric, and D.M. Engman, *Molecular mechanisms of protein and lipid targeting to ciliary membranes.* J Cell Sci, 2010. **123**(Pt 4): p. 529-36.
3. Rohatgi, R. and W.J. Snell, *The ciliary membrane.* Curr Opin Cell Biol, 2010. **22**(4): p. 541-6.
4. Pedersen, L.B. and J.L. Rosenbaum, *Intraflagellar transport (IFT) role in ciliary assembly, resorption and signalling.* Curr Top Dev Biol, 2008. **85**: p. 23-61.
5. Verhey, K.J., J. Dishinger, and H.L. Kee, *Kinesin motors and primary cilia.* Biochem Soc Trans, 2011. **39**(5): p. 1120-5.
6. Brown, J.M. and G.B. Witman, *Cilia and Diseases.* Bioscience, 2014. **64**(12): p. 1126-1137.
7. Rosenbaum, J.L. and G.B. Witman, *Intraflagellar transport.* Nat Rev Mol Cell Biol, 2002. **3**(11): p. 813-25.
8. Kotsis, F., C. Boehlke, and E.W. Kuehn, *The ciliary flow sensor and polycystic kidney disease.* Nephrol Dial Transplant, 2013. **28**(3): p. 518-26.
9. Nonaka, S., et al., *Determination of left-right patterning of the mouse embryo by artificial nodal flow.* Nature, 2002. **418**(6893): p. 96-9.
10. McGrath, J., et al., *Two populations of node monocilia initiate left-right asymmetry in the mouse.* Cell, 2003. **114**(1): p. 61-73.
11. Nauli, S.M., et al., *Polycystins 1 and 2 mediate mechanosensation in the primary cilium of kidney cells.* Nat Genet, 2003. **33**(2): p. 129-37.
12. Pazour, G. and J. Rosenbaum, *Intraflagellar transport and cilia-dependent diseases.* Trends Cell Biol, 2002. **12**(12): p. 551-5.
13. Paysan, J. and H. Breer, *Molecular physiology of odor detection: current views.* Pflugers Arch, 2001. **441**(5): p. 579-86.
14. Pazour, G.J., et al., *Chlamydomonas IFT88 and its mouse homologue, polycystic kidney disease gene tg737, are required for assembly of cilia and flagella.* J Cell Biol, 2000. **151**(3): p. 709-18.
15. Yoder, B., X. Hou, and L. Guay-Woodford, *The polycystic kidney disease proteins, polycystin-1, polycystin-2, polaris, and cystin, are co-localized in renal cilia.* J Am Soc Nephrol, 2002. **13**(10): p. 2508-16.
16. Pazour, G.J., *Intraflagellar transport and cilia-dependent renal disease: the ciliary hypothesis of polycystic kidney disease.* J Am Soc Nephrol, 2004. **15**(10): p. 2528-36.
17. Badano, J.L., et al., *The ciliopathies: an emerging class of human genetic disorders.* Annu Rev Genomics Hum Genet, 2006. **7**: p. 125-48.
18. Hildebrandt, F., M. Attanasio, and E. Otto, *Nephronophthisis: disease mechanisms of a ciliopathy.* J Am Soc Nephrol, 2009. **20**(1): p. 23-35.

19. Kerkar, N., K. Norton, and F.J. Suchy, *The hepatic fibrocystic diseases.* Clin Liver Dis, 2006. **10**(1): p. 55-71, v-vi.
20. Gunay-Aygun, M., *Liver and kidney disease in ciliopathies.* Am J Med Genet C Semin Med Genet, 2009. **151C**(4): p. 296-306.
21. Harris, P.C., *2008 Homer W. Smith Award: insights into the pathogenesis of polycystic kidney disease from gene discovery.* J Am Soc Nephrol, 2009. **20**(6): p. 1188-98.
22. Zerres, K., et al., *Prenatal diagnosis of autosomal recessive polycystic kidney disease (ARPKD): molecular genetics, clinical experience, and fetal morphology.* Am J Med Genet, 1998. **76**(2): p. 137-44.
23. Kaariainen, H., *Polycystic kidney disease in children: a genetic and epidemiological study of 82 Finnish patients.* J Med Genet, 1987. **24**(8): p. 474-81.
24. Lambie, L., et al., *Clinical and genetic characterization of a founder PKHD1 mutation in Afrikaners with ARPKD.* Pediatr Nephrol, 2015. **30**(2): p. 273-9.
25. Reuss, A., J.W. Wladimiroff, and M.F. Niermeyer, *Sonographic, clinical and genetic aspects of prenatal diagnosis of cystic kidney disease.* Ultrasound Med Biol, 1991. **17**(7): p. 687-94.
26. Bergmann, C., et al., *Clinical consequences of PKHD1 mutations in 164 patients with autosomal-recessive polycystic kidney disease (ARPKD).* Kidney Int, 2005. **67**(3): p. 829-48.
27. Guay-Woodford, L.M. and R.A. Desmond, *Autosomal recessive polycystic kidney disease: the clinical experience in North America.* Pediatrics, 2003. **111**(5 Pt 1): p. 1072-80.
28. Hartung, E.A. and L.M. Guay-Woodford, *Autosomal recessive polycystic kidney disease: a hepatorenal fibrocystic disorder with pleiotropic effects.* Pediatrics, 2014. **134**(3): p. e833-45.
29. Wen, J., *Congenital hepatic fibrosis in autosomal recessive polycystic kidney disease.* Clin Transl Sci, 2011. **4**(6): p. 460-5.
30. Srinath, A. and B.L. Shneider, *Congenital hepatic fibrosis and autosomal recessive polycystic kidney disease.* J Pediatr Gastroenterol Nutr, 2012. **54**(5): p. 580-7.
31. Gagnadoux, M.F., et al., *Cystic renal diseases in children.* Adv Nephrol Necker Hosp, 1989. **18**: p. 33-57.
32. Adeva, M., et al., *Clinical and molecular characterization defines a broadened spectrum of autosomal recessive polycystic kidney disease (ARPKD).* Medicine (Baltimore), 2006. **85**(1): p. 1-21.
33. Lilova, M., B.S. Kaplan, and K.E. Meyers, *Recombinant human growth hormone therapy in autosomal recessive polycystic kidney disease.* Pediatr Nephrol, 2003. **18**(1): p. 57-61.
34. Konrad, M., et al., *Body growth in children with polycystic kidney disease. Arbeitsgemeinschaft fur Padiatrische Nephrologie.* Acta Paediatr, 1995. **84**(11): p. 1227-32.
35. Zerres, K., et al., *Autosomal recessive polycystic kidney disease in 115 children: clinical presentation, course and influence of gender. Arbeitsgemeinschaft fur Padiatrische, Nephrologie.* Acta Paediatr, 1996. **85**(4): p. 437-45.

36. Capisonda, R., et al., *Autosomal recessive polycystic kidney disease: outcomes from a single-center experience.* Pediatr Nephrol, 2003. **18**(2): p. 119-26.
37. Dias, N.F., et al., *Clinical aspects of autosomal recessive polycystic kidney disease.* J Bras Nefrol, 2010. **32**(3): p. 263-7.
38. Neumann, H.P., et al., *Multiple intracranial aneurysms in a patient with autosomal recessive polycystic kidney disease.* Nephrol Dial Transplant, 1999. **14**(4): p. 936-9.
39. Lilova, M.I. and D.L. Petkov, *Intracranial aneurysms in a child with autosomal recessive polycystic kidney disease.* Pediatr Nephrol, 2001. **16**(12): p. 1030-2.
40. Chalhoub, V., et al., *Intracranial aneurysm and recessive polycystic kidney disease: the third reported case.* JAMA Neurol, 2013. **70**(1): p. 114-6.
41. Onuchic, L., et al., *PKHD1, the polycystic kidney and hepatic disease 1 gene, encodes a novel large protein containing multiple immunoglobulin-like plexin-transcription-factor domains and parallel beta-helix 1 repeats.* Am J Hum Genet, 2002. **70**(5): p. 1305-17.
42. Boddu, R., et al., *Intragenic motifs regulate the transcriptional complexity of Pkhd1/PKHD1.* J Mol Med (Berl), 2014. **92**(10): p. 1045-56.
43. Menezes, L.F., et al., *Polyductin, the PKHD1 gene product, comprises isoforms expressed in plasma membrane, primary cilium, and cytoplasm.* Kidney Int, 2004. **66**(4): p. 1345-55.
44. Nagasawa, Y., et al., *Identification and characterization of Pkhd1, the mouse orthologue of the human ARPKD gene.* J Am Soc Nephrol, 2002. **13**(9): p. 2246-58.
45. Guay-Woodford, L.M., *Autosomal recessive polycystic kidney disease: the prototype of the hepato-renal fibrocystic diseases.* J Pediatr Genet, 2014. **3**(2): p. 89-101.
46. O'Connor, A.K. and L.M. Guay-Woodford, *Polycystic Kidney Disease and Other Hepatorenal Fibrocystic Diseases: Clinical Phenotypes, Molecular Pathobiology, and Variation Between Mouse and Man*, in *Kidney Development, Disease, Repair, and Regernation*, M. Little, Editor 2015, Elsevier: San Diego, California, USA.
47. Ward, C.J., et al., *The gene mutated in autosomal recessive polycystic kidney disease encodes a large, receptor-like protein.* Nat Genet, 2002. **30**(3): p. 259-69.
48. Zhang, M.Z., et al., *PKHD1 protein encoded by the gene for autosomal recessive polycystic kidney disease associates with basal bodies and primary cilia in renal epithelial cells.* Proc Natl Acad Sci U S A, 2004. **101**(8): p. 2311-6.
49. Ward, C.J., et al., *Cellular and subcellular localization of the ARPKD protein; fibrocystin is expressed on primary cilia.* Hum Mol Genet, 2003. **12**(20): p. 2703-10.
50. Wang, S., et al., *The autosomal recessive polycystic kidney disease protein is localized to primary cilia, with concentration in the basal body area.* J Am Soc Nephrol, 2004. **15**(3): p. 592-602.
51. Bakeberg, J.L., et al., *Epitope-tagged Pkhd1 tracks the processing, secretion, and localization of fibrocystin.* J Am Soc Nephrol, 2011. **22**(12): p. 2266-77.
52. Gallagher, A.R., et al., *Biliary and pancreatic dysgenesis in mice harboring a mutation in Pkhd1.* Am J Pathol, 2008. **172**(2): p. 417-29.

53. Bertuccio, C.A. and M.J. Caplan, *Polycystin-1C terminus cleavage and its relation with polycystin-2, two proteins involved in polycystic kidney disease.* Medicina (B Aires), 2013. **73**(2): p. 155-62.
54. Kim, I., et al., *Fibrocystin/polyductin modulates renal tubular formation by regulating polycystin-2 expression and function.* J Am Soc Nephrol, 2008. **19**(3): p. 455-68.
55. Kaimori, J.Y., et al., *Polyductin undergoes notch-like processing and regulated release from primary cilia.* Hum Mol Genet, 2007. **16**(8): p. 942-56.
56. Gunay-Aygun, M., et al., *Correlation of kidney function, volume and imaging findings, and PKHD1 mutations in 73 patients with autosomal recessive polycystic kidney disease.* Clin J Am Soc Nephrol, 2010. **5**(6): p. 972-84.
57. Bergmann, C., et al., *PKHD1 mutations in autosomal recessive polycystic kidney disease (ARPKD).* Hum Mutat, 2004. **23**(5): p. 453-63.
58. Bergmann, C., et al., *Spectrum of mutations in the gene for autosomal recessive polycystic kidney disease (ARPKD/PKHD1).* J Am Soc Nephrol, 2003. **14**(1): p. 76-89.
59. Furu, L., et al., *Milder presentation of recessive polycystic kidney disease requires presence of amino acid substitution mutations.* J Am Soc Nephrol, 2003. **14**(8): p. 2004-14.
60. Bergmann, C., et al., *PKHD1 mutations in families requesting prenatal diagnosis for autosomal recessive polycystic kidney disease (ARPKD).* Hum Mutat, 2004. **23**(5): p. 487-95.
61. Sharp, A.M., et al., *Comprehensive genomic analysis of PKHD1 mutations in ARPKD cohorts.* J Med Genet, 2005. **42**(4): p. 336-49.
62. Zvereff, V., et al., *Identification of PKHD1 multiexon deletions using multiplex ligation-dependent probe amplification and quantitative polymerase chain reaction.* Genet Test Mol Biomarkers, 2010. **14**(4): p. 505-10.
63. Guay-Woodford, L.M., et al., *Consensus expert recommendations for the diagnosis and management of autosomal recessive polycystic kidney disease: report of an international conference.* J Pediatr, 2014. **165**(3): p. 611-7.
64. Denamur, E., et al., *Genotype-phenotype correlations in fetuses and neonates with autosomal recessive polycystic kidney disease.* Kidney Int, 2010. **77**(4): p. 350-8.
65. Lager, D.J., et al., *The pck rat: a new model that resembles human autosomal dominant polycystic kidney and liver disease.* Kidney Int, 2001. **59**(1): p. 126-36.
66. Williams, S.S., et al., *Kidney cysts, pancreatic cysts, and biliary disease in a mouse model of autosomal recessive polycystic kidney disease.* Pediatr Nephrol, 2008. **23**(5): p. 733-41.
67. O'Meara, C.C., et al., *Role of genetic modifiers in an orthologous rat model of ARPKD.* Physiol Genomics, 2012. **44**(15): p. 741-53.
68. Garcia-Gonzalez, M., et al., *Genetic interaction studies link autosomal dominant and recessive polycystic kidney disease in a common pathway.* Hum Mol Genet, 2007. **16**(16): p. 1940-50.
69. Cogswell, C., et al., *Positional cloning of jcpk/bpk locus of the mouse.* Mamm Genome, 2003. **14**(4): p. 242-9.
70. Hou, X., et al., *Cystin, a novel cilia-associated protein, is disrupted in the cpk mouse model of polycystic kidney disease.* J Clin Invest, 2002. **109**(4): p. 533-40.

71. Tao, B., et al., *Cystin localizes to primary cilia via membrane microdomains and a targeting motif.* J Am Soc Nephrol, 2009. **20**(12): p. 2570-80.
72. Wu, M., et al., *The ciliary protein cystin forms a regulatory complex with necdin to modulate Myc expression.* PLoS One, 2013. **8**(12): p. e83062.
73. McLaughlin, S. and A. Aderem, *The myristoyl-electrostatic switch: a modulator of reversible protein-membrane interactions.* Trends Biochem Sci, 1995. **20**(7): p. 272-6.
74. Cowley, B.J., et al., *Elevated proto-oncogene expression in polycystic kidneys of the C57BL/6J (cpk) mouse.* J Am Soc Nephrol, 1991. **1**(8): p. 1048-53.
75. Burn, T.C., et al., *Increased exon-trapping efficiency through modifications to the pSPL3 splicing vector.* Gene, 1995. **161**(2): p. 183-7.
76. Ramirez-Solis, R., P. Liu, and A. Bradley, *Chromosome engineering in mice.* Nature, 1995. **378**(6558): p. 720-4.
77. Smith, A.J., et al., *A site-directed chromosomal translocation induced in embryonic stem cells by Cre-loxP recombination.* Nat Genet, 1995. **9**(4): p. 376-85.
78. Perez, I., et al., *Mutation of PTB binding sites causes misregulation of alternative 3' splice site selection in vivo.* RNA, 1997. **3**(7): p. 764-78.
79. Cleary, M.A., et al., *Disruption of an imprinted gene cluster by a targeted chromosomal translocation in mice.* Nat Genet, 2001. **29**(1): p. 78-82.
80. Valenzuela, D.M., et al., *High-throughput engineering of the mouse genome coupled with high-resolution expression analysis.* Nat Biotechnol, 2003. **21**(6): p. 652-9.
81. Yeo, G., et al., *Variation in sequence and organization of splicing regulatory elements in vertebrate genes.* Proc Natl Acad Sci U S A, 2004. **101**(44): p. 15700-5.
82. Yeo, G.W., et al., *Identification and analysis of alternative splicing events conserved in human and mouse.* Proc Natl Acad Sci U S A, 2005. **102**(8): p. 2850-5.
83. Skarnes, W.C., et al., *A conditional knockout resource for the genome-wide study of mouse gene function.* Nature, 2011. **474**(7351): p. 337-42.
84. Dishinger, J.F., et al., *Ciliary entry of the kinesin-2 motor KIF17 is regulated by importin-beta2 and RanGTP.* Nat Cell Biol, 2010. **12**(7): p. 703-10.
85. Hurd, T.W., S. Fan, and B.L. Margolis, *Localization of retinitis pigmentosa 2 to cilia is regulated by Importin beta2.* J Cell Sci, 2011. **124**(Pt 5): p. 718-26.
86. Sorokin, S.P., *Reconstructions of centriole formation and ciliogenesis in mammalian lungs.* J Cell Sci, 1968. **3**(2): p. 207-30.
87. Field, M.C. and M. Carrington, *The trypanosome flagellar pocket.* Nat Rev Microbiol, 2009. **7**(11): p. 775-86.
88. Overath, P. and M. Engstler, *Endocytosis, membrane recycling and sorting of GPI-anchored proteins: Trypanosoma brucei as a model system.* Mol Microbiol, 2004. **53**(3): p. 735-44.
89. Benmerah, A., *The ciliary pocket.* Curr Opin Cell Biol, 2013. **25**(1): p. 78-84.
90. Ghossoub, R., et al., *The ciliary pocket: a once-forgotten membrane domain at the base of cilia.* Biol Cell, 2011. **103**(3): p. 131-44.

91. Molla-Herman, A., et al., *The ciliary pocket: an endocytic membrane domain at the base of primary and motile cilia.* J Cell Sci, 2010. **123**(Pt 10): p. 1785-95.
92. Owen, D.J., B.M. Collins, and P.R. Evans, *Adaptors for clathrin coats: structure and function.* Annu Rev Cell Dev Biol, 2004. **20**: p. 153-91.
93. Traub, L.M., *Tickets to ride: selecting cargo for clathrin-regulated internalization.* Nat Rev Mol Cell Biol, 2009. **10**(9): p. 583-96.
94. Hutagalung, A.H. and P.J. Novick, *Role of Rab GTPases in membrane traffic and cell physiology.* Physiol Rev, 2011. **91**(1): p. 119-49.
95. Schrick, J.J., et al., *ADP-ribosylation factor-like 3 is involved in kidney and photoreceptor development.* Am J Pathol, 2006. **168**(4): p. 1288-98.
96. Wright, K.J., et al., *An ARL3-UNC119-RP2 GTPase cycle targets myristoylated NPHP3 to the primary cilium.* Genes Dev, 2011. **25**(22): p. 2347-60.